PHYSICAL REVIEW D VOLUME 43, NUMBER 1 1 JANUARY 1991

Effective-Lagrangian approach to the theory of pion photoproduction in the Δ(1232) region

R. M. Davidson,* Nimai C. Mukhopadhyay, and R. S. Wittman†
Physics Department, Rensselaer Polytechnic Institute, Troy, New York 12180-3590
(Received 11 September 1989)

We investigate theoretical uncertainties and model dependence in the extraction of the nucleon-Δ(1232) electromagnetic transition amplitudes from the multipole data base. Our starting point is an effective Lagrangian incorporating chiral symmetry, which includes, at the tree level, the pseudovector nucleon Born terms, leading t-channel vector-meson exchanges, and s- and u-channel Δ exchanges. We express the nucleon-Δ transition magnetic dipole ($M1$) and electric quadrupole ($E2$) amplitudes in terms of two independent gauge couplings at the $\gamma N\Delta$ vertex, and fit these to various multipole data sets. We find a large sensitivity to the method used in unitarizing the amplitude, and extract the $E2/M1$ ratio (EMR) to be *negative,* with a magnitude of around 1.5%. The resonant amplitudes in this work are of interest to the test of topical hadron models inspired by QCD: the sign of the EMR, extracted by us, is in accord with that predicted by most realistic models, and its magnitude lies between the predictions of the quark shell model and the Skyrmion model. Finally, our work provides a phenomenologically satisfying unitary amplitude for pion photoproduction off nucleons, which can be used as a realistic starting point for theoretical studies of this process in complex nuclei.

I. INTRODUCTION

With the advent of quantum chromodynamics (QCD) as the theoretical framework of the strong interactions in the standard model, the spectroscopy of hadrons has taken a new importance[1] in the context of the application of QCD to describe the structure of hadrons. In the nonperturbative domain, however, QCD is very difficult to apply directly to this problem. Only for heavy mesons are lattice calculations beginning to give some insight into rigorous results. A comprehensive treatment of hadron spectroscopy in the framework of QCD is still far away, and the current generation of models can only build some aspects of it into their basic structure. Hence the adjective "QCD inspired" is often used to describe these often imperfect models.

In this quest for better applications of QCD, electroweak transition amplitudes are beginning to provide powerful tests[1] of the quality of emerging models. Thus, for excited-baryon spectroscopy, there is a continuing need to determine accurately the three-point function γNN^* (N denotes nucleon and N^* an excited baryon), from the experimental data of increasingly superior quality, and to contrast them with their best theoretical estimates. To this end, a new generation of "medium-energy" accelerators, such as the Continuous Electron Beam Accelerator Facility (CEBAF) in Virginia, are being built to complement the high-energy facilities. In the former, continuous-wave (cw), electrons will be available. Thus, it will soon be possible to study γNN^* vertices with polarized hadron targets and polarized electron or photon beams with high precision. In facilities such as the Brookhaven Laser-Electron-Gamma Source (LEGS), the photon polarization is nearly 100% and can be varied at will. This exciting experimental prospect calls for a careful theoretical examination of the vast data already available.[2] Our work here is an example of this effort[3,4] in the Δ(1232) region.

Discovered first, the Δ(1232) resonance enjoys a special place in the family of baryon resonances. Its structure has interesting features in the nonrelativistic quark model: to give one example, the nucleon-Δ mass splitting is a measure of the color-hyperfine interaction among the quarks. The nucleon-to-Δ electromagnetic transition, which can be magnetic dipole ($M1$) or electric quadrupole ($E2$), is, in the simplest version of the nonrelativistic quark model, a direct determinant of the role of the color-magnetic interaction, which gives rise to a small, but nonvanishing, $E2$ transition amplitude.[5] This is in sharp contrast to the virtual-photon three-point function $\gamma_v NN^*$ in the domain of perturbative QCD: there the $E2$ and $M1$ amplitudes are predicted[6] to be equal, this being a hundredfold increase in the ratio of the $E2$ to $M1$ amplitudes and a change of their relative sign. Thus, testing both of these predictions is an important goal in our understanding of hadron structure in the two distinct domains of QCD.

In this paper we are concerned with the *real-photon* piece of that test. The electromagnetic transition amplitudes are also of special interest to other models of hadrons such as deformed bags,[7] Skyrmions,[8] hybrids,[9] and so forth. From the point of view of extracting the resonant amplitude from data on photoproduction of pions, the Δ(1232) resonance offers an important simplification: its strong decay is only via the πN channel. Our objective in this theoretical paper will be to exploit this simplicity and examine the theoretical problems involved in the extraction of the $N\rightarrow\Delta$ resonant amplitudes from the vast data already in literature. Results obtained in this work should thus be of immediate interest to particle physicists in the following way: hadron-structure theorists can get a feeling for the magnitude of *theoretical un-*

certainty in extracting the $\gamma N\Delta$ amplitudes from the extant *experimental data.* The experimentalists, planning better studies on this problem at the emerging medium-energy electron or photon facilities, should get a hint on which specific observables need to be determined with improved precisions, to aid further the quality of extraction of the resonant $\gamma N\Delta$ amplitudes. Finally, our work here is of relevance to the studies of pion photoproduction off complex nuclei, wherein a satisfactory impulse amplitude for the process on a single nucleon is the starting point[10] of the theoretical description.

In this paper we examine pion photoproduction from threshold through the $\Delta(1232$ MeV) resonance region in the framework of an effective-Lagrangian approach,[11,12] following and extending the works of Olsson and Osypowski.[13] We are thus able to investigate both resonant and background pion-photoproduction mechanisms. We also address many of the ambiguities associated with the effective-Lagrangian approach. The effective Lagrangian uses the pseudovector (PV) coupling in the nucleon Born amplitudes, and thus incorporates the low-energy theorems[14] of current algebra and the hypothesis of partially conserved axial-vector current (PCAC). The off-shell ambiguity[15] of the massive spin-$\frac{3}{2}$ field is exploited in this approach by introducing three allowed arbitrary parameters (the off-shell parameters), one for each of the two $\gamma N\Delta$ vertices and one for the $\pi N\Delta$ vertex. This generalizes the procedure of Olsson and Osypowski,[13] who first emphasized differences of this approach from the dispersion theoretic ones.[16] The ease of incorporating low-energy theorems, investigating the possible role of t-channel vector-meson exchanges without serious double counting and without violating the low-energy theorems,[13,17] and a treatment of Δ-resonance propagation in a more general way than the Breit-Wigner form,[18] are three important features of the Olsson-type approaches.

One important extension of the Olsson formalism is the inclusion of two independent gauge couplings, $g_{1\Delta}$ and $g_{2\Delta}$, at the $\gamma N\Delta$ vertex [see Eqs. (12) and (13)]. Nath and Bhattacharyya[19] (NB) have recently argued that it is not possible, for any value of the off-shell parameter, to derive eight Pauli-Fierz-type constraints for an elementary spin-$\frac{3}{2}$ field, and the $g_{1\Delta}$ and $\pi N\Delta$ couplings are compatible with these constraints only for *specific values* of the off-shell parameters. One of the objectives of this paper is to test this contention of NB, in view of the theoretical questions as to whether the NB conjecture is applicable to an extended particle (such as Δ). We have found that setting $g_{2\Delta}=0$ fails to reproduce the E_{1+} $(T=\frac{3}{2})$ multipole (due to an $E2$ photon), and thus we have adopted the attitude of Olsson and fitted $g_{1\Delta}$ and $g_{2\Delta}$ and the off-shell parameters to the data.

Since one of our main objectives is to investigate the model dependence in the extraction of the electromagnetic transition amplitudes from the data, freedom in the gauge coupling is absolutely essential for the determination from the multipole data of a possible electric quadrupole ($E2$) contribution to the $\gamma N\Delta$ transition amplitude, a subject of considerable current interest[1] in the theory of hadron structure. It also turns out to be of some importance in the discussion[20] of neutral-pion photoproduction *below* the charged-pion threshold, on which experimental data[21] from Saclay and Mainz have become recently available, and caused considerable excitement in the particle-physics community due to their apparent disagreement with the predictions of the low-energy theorems and their extensions.

We also differ from Olsson by considering a variety of unitarization procedures (of which the Olsson ansatz[18] is a special case), and their effects on the extraction of the resonant $\gamma N\Delta$ transition amplitudes. This is interesting for exploring the model dependence introduced by the unitarization recipes in determining the resonant amplitudes, and their phenomenological successes as given by the quality of corresponding multipole fits. We examine the possible energy dependence of the unknown parameters, particularly in the resonant sector, by choosing the multipoles to be fitted in different energy regions. Finally, we fit different multipole sets available in the literature,[22–26] with primary emphasis on fitting those of Pfeil and Schwela[23] (PS), and Berends and Donnachie[22] (BD) because of their completeness in information. We also take into account the new data bases[24–26] added to these rather complete, but dated analyses. This allows us to infer the differences inherent in various extant multipole sets, and draw some conclusions on future directions of better multipole analyses.

As we have already indicated, our two primary objectives are to examine the model dependence of the extraction of the resonant $\gamma N\Delta$ amplitudes from the existing multipole data and to provide a unitary theory for the pion photoproduction from nucleons for application in complex nuclei. Our work has already exposed[10] limitations of nonunitary impulse operators[27] in use before our work. Here we will not discuss implementation of our amplitude into a nuclear calculation. While the theoretical understanding of pion photoproduction in complex nuclei in the first resonance region is not yet complete, primarily due to the lack of treating the role of pionic single-charge-exchange reactions and the possible medium modifications of the impulse operator in a single theoretical framework, our present work provides a key ingredient in that process. Tremendous experimental progress[28] at the current generation of electron accelerators, and continued expectation of better quality experiments at the newer cw machines provides a strong challenge for further theoretical understanding of the complex nuclear processes.

This work has important differences with our earlier works[4,29] on the $\gamma N\Delta$ transition amplitudes. In Ref. 29, two of us extracted, in a model-independent fashion, the K-matrix residues in the Δ region. Although these are important quantities, they provide information for only two multipoles (the E_{1+} and M_{1+}, both $T=\frac{3}{2}$) and at only one energy, whereas we also want to understand the entire pion-photoproduction amplitude from threshold through the Δ region. We emphasize that the transition amplitudes we obtain here are *model dependent,* in contrast with those of Ref. 29, but the spread of values obtained from different unitarization methods give us a measure of the theoretical uncertainties in extracting the

helicity amplitudes for the $\gamma N \leftrightarrow \Delta$ transition from the data, needed in comparing with hadron model calculations of the transition amplitudes. Finally, we supersede our earlier work[3,4] by considering several data sets, several unitarization methods, and a more realistic background contribution.

The remainder of this paper is organized as follows. Section II contains our main theoretical discussion on how we structure our analysis. Sections III and IV are interdependent: they comprise the results of our analysis and their critical discussions, respectively. Section V details a summary of our conclusions. Some technical details of our calculation, helpful for relating our work to others in the literature, are contained in the Appendix.

II. FORMALISM: VARIOUS ASPECTS OF OUR THEORETICAL ANALYSIS

A. $\gamma N \Delta$ transition amplitudes

The electromagnetic transition from the nucleon ($\frac{1}{2}^+$, $T=\frac{1}{2}$) to the Δ ($\frac{3}{2}^+$, $T=\frac{3}{2}$) can be either magnetic dipole ($M1$) or electric quadrupole ($E2$). Based on Lorentz invariance and gauge invariance, we may write the matrix element for this transition:

$$iM_{fi}=\frac{e}{2M}\bar{u}_n\tilde{\tau}_3\gamma_5\left[g_{1\Delta}(\gamma\cdot k\,\epsilon_\nu-\gamma\cdot\epsilon\,k_\nu)+\frac{g_{2\Delta}}{2M}(P_n\cdot\epsilon\,k_\nu-P_n\cdot k\,\epsilon_\nu)\right]u^\nu_\Delta\ , \quad (1)$$

where M is the nucleon mass, k is the photon four-momentum, P_n is the nucleon four-momentum, ϵ_μ is the photon polarization, u_n is the nucleon spinor, u^ν_Δ is the Δ vector-spinor, and $\tilde{\tau}_3$ is the $\frac{3}{2}\leftrightarrow\frac{1}{2}$ isospin transition matrix. We note that there are other definitions[30] of iM_{fi}, but they are equivalent when the baryons are on shell.

In the conventions of the Particle Data Group,[31] we can write the electromagnetic transition amplitudes as

$$E2=\frac{-e}{6M}\frac{k_\Delta}{(M_\Delta+M)}\left[\frac{k_\Delta M_\Delta}{M}\right]^{1/2}\left[g_{1\Delta}-\frac{g_{2\Delta}M_\Delta}{2M}\right], \quad (2)$$

and

$$M1=\frac{e}{12M}\left[\frac{k_\Delta}{M_\Delta M}\right]^{1/2}\left[g_{1\Delta}(3M_\Delta+M)-g_{2\Delta}\frac{M_\Delta(M_\Delta-M)}{2M}\right]. \quad (3)$$

The electromagnetic partial widths, using typical values of $M1$ and $E2$ amplitudes extracted in this work, are

$$\Gamma_{M1}=\frac{k_\Delta^2 M(M1)^2}{2\pi M_\Delta}\approx\tfrac{1}{2}\text{ MeV}\ , \quad (4)$$

$$\Gamma_{E2}=\frac{3k_\Delta^2 M(E2)^2}{2\pi M_\Delta}\approx 2\times10^{-4}\text{ MeV}\ , \quad (5)$$

where $k_\Delta=(M_\Delta^2-M^2)/2M_\Delta$, M_Δ being the mass of the Δ. Recall that the πN decay width is about 100 MeV. The helicity amplitudes are related to $E2$ and $M1$ by

$$A_{1/2}=-\tfrac{1}{2}(M1+3E2)\ , \quad (6)$$

$$A_{3/2}=-\frac{\sqrt{3}}{2}(M1-E2)\ . \quad (7)$$

As we have pointed out earlier, there is considerable discussion in the recent literature on the parameter $g_{2\Delta}$. Many authors[13,27] have set $g_{2\Delta}=0$, but if the $E2$ and $M1$ are to be independent, $g_{2\Delta}$ must be kept arbitrary. It has to be determined, along with $g_{1\Delta}$, by a fit to the multipole data. In fact, from Eqs. (2)–(5), we find $g_{1\Delta}\approx 5$, and $g_{2\Delta}\approx 6$. If $g_{2\Delta}=0$, then we would obtain the result $E2/M1=-(M_\Delta-M)/(3M_\Delta+M)\approx -6\%$, whereas our extracted values for $E2/M1$ are $\approx -1.5\%$.

Another point about Eqs. (2) and (3) is that $E2$ and $M1$ depend on M_Δ. Different parametrizations of the δ_{33}, the phase shift in the 33 channel in πN elastic scattering, give values for M_Δ ranging from 1215 to 1250 MeV, and the fits to the data are roughly equivalent. Fortunately the uncertainty in $E2$ and $M1$ due to that in M_Δ is not large. One might also consider using the T-matrix pole position for M_Δ (which is complex), thereby making the $E2$ and $M1$ amplitudes complex. While more detailed calculations might give complex $E2$ and $M1$, as some authors show,[32] the current generation of baryon models predict real $E2$ and $M1$. Since we want to provide constraints for these models, we assume M_Δ to be real and to lie in the range $1215<M_\Delta<1250$. This illustrates that care must be taken in comparing the transition amplitudes extracted from the data with those predicted by baryon models.

B. Pion-photoproduction amplitude

The $E2$ and $M1$ depend on two parameters $g_{1\Delta}$ and $g_{2\Delta}$, which should be determined from the data. Here we focus on extracting the gauge couplings from the pion-photoproduction data. In the future we hope to be able to use the data on radiative pion capture and Compton scattering to constraint $g_{1\Delta}$ and $g_{2\Delta}$.

A general problem in any extraction of $N^*\leftrightarrow\gamma N$ amplitudes is the separation of the resonant and background contributions to pion photoproduction, and in the Δ resonance region, we may take advantage of the multipole data sets to test how well the background is known. The s-channel Δ exchange gives a *resonant* contribution only to the M_{1+} ($T=\frac{3}{2}$) and E_{1+} ($T=\frac{3}{2}$) multipoles. We use the standard definitions and notations for the multipoles.[16,33] These multipoles also contain background contributions: in our effective-Lagrangian approach, the physics of the background contribution can be tested by its success in predicting *other nonresonant multipoles.*

Olsson and Osypowski[13] have previously investigated the background contributions to the (γ,π) amplitude in the Δ resonance region. They found that the following contributions give a good account of the nonresonant multipoles (all multipoles except the $E_{1+}^{3/2}$ and the $M_{1+}^{3/2}$).

(1) Pseudovector (PV) nucleon Born terms.

(2) t-channel ω and ρ exchange.

(3) Nonresonant Δ exchange. This includes the crossed, or u channel, Δ exchange as well as contributions from the spin-$\frac{1}{2}$ part of the Δ field.[34]

The amplitudes for the PV nucleon Born terms are well known, and are given in the Appendix for completeness. There are a few important items to note.

(1) The PV nucleon Born terms generally dominate the background and contribute to all multipoles. There are no free parameters for these terms.

(2) We have not introduced any form factors into the amplitude and the Born terms are gauge invariant. One can make use of the form factors at various vertices, but this would require special care to maintain gauge invariance. In our fits, we are not forced to use explicit form factors. We discuss this point further in Secs. II D and IV B.

(3) We have found that other single-particle exchanges are small in the energy region of interest here, due primarily to smaller photon and/or pion coupling strengths, and the fact that other resonances are far away. There is also the possibility of a σ term[35] contributing to the S waves (S,P, etc. refer to the pion-nucleon relative angular momentum), which we have ignored since for isospin $\frac{1}{2}$ and $\frac{3}{2}$ it is expected to be small. This is because the E_{0+} ($T=\frac{1}{2},\frac{3}{2}$) multipoles are dominated by the Kroll-Ruderman[36] term arising in charged-pion production. However, it is expected[35] to be of some importance in threshold π^0 production.

The effective Lagrangian we use for t-channel ω and ρ exchange is

$$L=\frac{e\lambda_V}{4m}\epsilon_{\mu\nu\lambda\sigma}F^{\mu\nu}V^{\lambda\sigma}\Pi-g_{V1}\bar{N}\gamma_\mu V^\mu+\frac{g_{V2}}{4M}\bar{N}\sigma_{\mu\nu}NV^{\mu\nu}\ , \tag{8}$$

where V^μ is the ρ or ω field, Π is the pion field, N is the nucleon field, $F^{\mu\nu}$ is the electromagnetic field tensor, and $V^{\lambda\sigma}\equiv\partial^\sigma V^\lambda-\partial^\lambda V^\sigma$; m is the pion mass.

The isospin content of the t-channel vector-meson exchange is such that ω contributes to the isovector amplitudes, and ρ contributes only to the isoscalar amplitudes. As a consequence of this, ρ exchange may be decoupled from the Δ exchange, since the Δ contributes only the $(+)$ and $(-)$ isovector amplitudes.

The radiative coupling λ_ν may be determined from the $V\to\pi\gamma$ decay width using

$$\Gamma_{V\to\pi\gamma}=\frac{e^2\lambda_V^2k^3}{12\pi m^2}\ , \tag{9}$$

where k is the photon three-momentum. From the data on radiative decays,[31] we get $\lambda_\omega=0.36$ and $\lambda_\rho=0.11$. For the strong couplings,[37] $g_{\rho1}\approx1.8-3.2$, $g_{\rho2}/g_{\rho1}\approx4.3-6.6$, $g_{\omega1}\approx8-14$, and $g_{\omega2}/g_{\omega1}\approx0-(-1)$. The vector-dominance predictions[38] are $g_{\rho2}/g_{\rho1}=(\kappa_p-\kappa_n)$ and $g_{\omega2}/g_{\omega1}=(\kappa_p+\kappa_n)$, where κ_p and κ_n are the anomalous magnetic moments of the proton and neutron, respectively.

We find that the pion-photoproduction data generally favors $g_{\omega2}\approx-g_{\omega1}$ rather than $g_{\omega2}\approx0$ (a result in agreement with Olsson and Osypowski[13]), but the value of $g_{\omega2}$ has little influence on the extracted values of the $E2$ and $M1$ amplitudes. We consider variations of the VNN couplings in the above range to test the sensitivity of the $E2$ and $M1$ amplitudes to the vector-meson exchanges.

C. Contributions to the amplitude involving Δ

The effective Lagrangian for the $\pi N\Delta$ interaction and the $\gamma N\Delta$ interaction[13] is

$$L=L_{\pi N\Delta}+L^1_{\gamma N\Delta}+L^2_{\gamma N\Delta}\ , \tag{10}$$

where

$$L_{\pi N\Delta}=\frac{g_{\pi N\Delta}}{m}(\partial^\mu\Pi)\bar{N}\tilde{\tau}O_{\mu\nu}(Z)\Delta^\nu+\text{H.c.}\ , \tag{11}$$

$$L^1_{\gamma N\Delta}=\frac{ieg_{1\Delta}}{2M}\bar{\Delta}^\mu O_{\mu\lambda}(Y)\gamma_\nu\gamma_5\tilde{\tau}^\dagger_3NF^{\nu\lambda}+\text{H.c.}\ , \tag{12}$$

$$L^2_{\gamma N\Delta}=\frac{-eg_{2\Delta}}{4M^2}\bar{\Delta}^\mu O_{\mu\nu}(X)\gamma_5\tilde{\tau}^\dagger_3(\partial_\lambda N)F^{\nu\lambda}+\text{H.c.}\ . \tag{13}$$

Here, Δ^μ is the Δ field, $\tilde{\tau}$ are the $\frac{1}{2}\leftrightarrow\frac{3}{2}$ isospin transition matrices (see the Appendix) and

$$O_{\mu\nu}(Z)=g_{\mu\nu}+[\tfrac{1}{2}(1+4Z)A+Z]\gamma_\mu\gamma_\nu\ . \tag{14}$$

This interaction has been extensively discussed in the literature.[12,19] The form of $O_{\mu\nu}$ has been chosen to give the most general Lagrangian (limited to the number of derivatives above) that obeys the same point transformation[39] as the free spin-$\frac{3}{2}$ Lagrangian. This guarantees that the parameter A that appears in $O_{\mu\nu}$ and in the propagator will not appear in any physical matrix element.[40]

The electromagnetic part of the Δ interaction Lagrangian reproduces the general transition amplitude, Eq. (1), when evaluated in the tree approximation. Note that Eq. (1) is independent of the off-shell parameters, which is consistent with the fact that the residues of the photoproduction amplitude in the tree approximation are also independent of the off-shell parameters. Nath and Bhattacharyya[19] have shown that problems occur with the field theory of point spin-$\frac{3}{2}$ particles unless $g_{2\Delta}=0$, $Z=\frac{1}{2}$, and $Y=0$. As we discussed earlier, this constrains the ratio $E2/M1$ to be $\approx-6\%$. We find that these constraints, particularly $g_{2\Delta}=0$, are much too restrictive for a *phenomenological* description of the spin $\frac{1}{2}\leftrightarrow\frac{3}{2}$ transitions between *composite* particles. We keep $g_{1\Delta}$ and $g_{2\Delta}$ as free parameters to be fitted to the multipole data. Finally, we note that the choices of Nath and Bhattacharyya of $g_{2\Delta}$, Z, and Y do not solve all the problems of interacting spin-$\frac{3}{2}$ fields. (An example of a consistent theory of interacting spin-$\frac{3}{2}$ particles is supergravity.[41])

The Δ exchange contains both resonant and nonresonant contributions. The nonresonant contributions come from the u-channel exchange, the spin-$\frac{1}{2}$ part of the Δ propagator, and the anti-Δ exchange. Thus, when the Δ-exchange contribution is decomposed into multipoles, all the isovector multipoles receive a contribution from it, indicating that $g_{1\Delta}$, $g_{2\Delta}$, X, Y, and Z must be fitted to all multipoles, for consistency. This is in contrast with previous works[4,42–44] where $g_{1\Delta}$ and $g_{2\Delta}$ were determined by

fitting just the resonant multipoles. In practice we have fitted only those multipoles with $l \leq 1$, l being the πN orbital angular momentum. This is dictated by the fact that most multipole analyses fit multipoles up to $l=1$, taking the nucleon Born terms for the higher partial waves. Recall that PV and pseudoscalar (PS) couplings give identical multipoles (in the tree approximation) for $l>1$.

D. Unitarity problem for the strong channel

The tree approximation yields real amplitudes and therefore violates unitarity, since Watson's theorem[45] requires the phase of the amplitude to be nonzero. Furthermore, the s-channel Δ exchange gives a pole on the real axis in the tree approximation. The common origin of these problems is the neglect the final-state interaction via pion-nucleon rescattering. While the problem of πN rescattering should be treated dynamically,[42–44] we follow the spirit of Olsson and implement unitarity phenomenologically, since no consistent *relativistic,* gauge-invariant, dynamical treatment of this problem, is yet available, despite many brave attempts[44] to improve the situation.

The unitarization of the pion-photoproduction amplitude is intimately related to the πN scattering, and therefore we first describe the unitarization of the tree approximation to πN elastic scattering in the Δ region. Our main purpose here is *not* to provide a model of πN scattering. We do note that it is possible to obtain the scattering lengths and volumes starting from an effective Lagrangian,[46] and δ_{33} can be accurately reproduced.[18]

The unitarization of the effective-Lagrangian amplitude is not unique, and for the *nonresonant* partial waves $f_{l\pm}$ (all partial waves except $f_{1+}^{3/2}$), our ansatz is

$$qf_{l\pm}^{TA}=\tan\delta_{l\pm} , \tag{15}$$

$$qf_{l\pm}=\sin\delta_{l\pm}e^{i\delta_{l\pm}} , \tag{16}$$

where $f_{l\pm}^{TA}$ is the tree approximation to the amplitude. This is equivalent to assuming that the tree approximation gives *K-matrix* elements with

$$\frac{qf_{l\pm}}{1+iqf_{l\pm}}=K_{l\pm}\equiv qf_{l\pm}^{TA}=\tan\delta_{l\pm} . \tag{17}$$

The unitarization methods used here can be viewed as procedures to account for the absorptive corrections from higher-order diagrams. It is assumed that the dispersive corrections only renormalize the masses and couplings to their physical values and that the variation in the masses and couplings away from their defining point can be ignored. Other authors[42–44] have also made *models* for the dispersive corrections. Weinberg[47] has outlined a framework within the context of a chiral-invariant effective Lagrangian whereby loops may be calculated. The important point is that in higher orders additional vertices appear, and Weinberg's approach is not equivalent to approaches that introduce a cutoff and iterate the PV-Born terms. Thus, in our opinion, the dispersive corrections in this problem are not yet well understood.

As noted above, the K-matrix approach can be used to reproduce the scattering lengths and volumes for πN elastic scattering. It would be interesting to know how well this approach reproduces the nonresonant phase shifts throughout the Δ region, but as far as our approach to *pion photoproduction* is concerned, the answer to this question is not too crucial. If the model fails at some point, as it must, we may always consider adding additional particle exchanges in order to improve agreement with the data. The important question in this model for pion photoproduction is whether the additional particles also contribute in the tree approximation to the (γ,π) amplitude. For example, our initial amplitude for πN scattering could come just from s- and u-channel nucleon exchange. To improve the model we could add a t-channel σ exchange, but since there is no $\sigma\pi\gamma$ coupling (violates C), there would be no t-channel σ contribution to pion photoproduction. Thus, we believe that we are considering all the important tree-level contributions to pion photoproduction in this energy region. There is also a theoretical problem[20] of accounting for the observed[21] π^0 photoproduction cross section near threshold. This may be connected to the last item we have just discussed.

To further illustrate our approach, consider the T matrix for pion photoproduction in terms of the K matrix (at the moment we are concerned with nonresonant partial waves and multipoles): $T=K(1+iT)$. Ignoring terms of order e^2,

$$T_{\gamma\pi}=K_{\gamma\pi}(1+iT_{\pi\pi}) , \tag{18}$$

or equivalently with $T_{\pi\pi}=\sin\delta_{\pi\pi}e^{i\delta_{\pi\pi}}$, we have

$$T_{\gamma\pi}=K_{\gamma\pi}\cos\delta_{\pi\pi}e^{i\delta_{\pi\pi}} , \tag{19}$$

where $\delta_{\pi\pi}$ is the πN scattering phase shift. The assumption we make is that $K_{\gamma\pi}$ is given by the tree approximation, and therefore we may use the *experimental* phase shifts as input to our pion-photoproduction calculation. We note, in Olsson's method of unitarization the following relation holds:

$$T_{\gamma\pi}=K_{\gamma\pi}e^{i\delta_{\pi\pi}} , \tag{20}$$

which differs from (19) by a $\cos\delta_{\pi\pi}$ term. Since $\delta_{\pi\pi}\lesssim 20°$ for the nonresonant phase shifts in the Δ region, this has less than a 10% effect on the nonresonant multipole amplitudes.

Although we can get away here without making a careful theory of nonresonant πN scattering, we must make a reasonable model for resonant πN scattering because the pion-photoproduction amplitude depends on $g_{\pi N\Delta}$ and M_Δ, which are strong-interaction parameters. The parameter Z in $L_{\pi N\Delta}$ can also be determined from πN scattering, but this would require making a model for nonresonant πN scattering. We fit Z to the pion-photoproduction data and compare it with the value obtained from an analysis of πN scattering by Olsson and Osypowski.[48]

The s-channel Δ contribution to πN scattering in the 33 channel is

$$qf_{1+}^{\Delta}=\frac{M_\Delta\Gamma_\Delta(s)}{M_\Delta^2-s}\equiv\frac{1}{\epsilon}\ , \tag{21}$$

where

$$\Gamma_\Delta(s)=\frac{g_{\pi N\Delta}^2(E_f+M)(W+M_\Delta)q^3}{24\pi m^2 W M_\Delta}\ . \tag{22}$$

There are also background contribution to $f_{1+}^{3/2}$, which we simply write as

$$qf_{1+}^{B}=\tan\delta_B\ . \tag{23}$$

We now consider the unitarization of the resonant πN partial wave in the Olsson,[18] Noelle,[49] and K-matrix approaches. These methods give

$$qf_{1+}=\tan\delta_{33}=\frac{1+\epsilon\tan\delta_B}{\epsilon+\eta\tan\delta_B}\ , \tag{24}$$

where $\eta=+1$ for the Olsson ansatz, -1 for the Noelle ansatz, and 0 for the K matrix ansatz. As we shall show, all three approaches give roughly equivalent fits to the δ_{33} phase shift and are in good agreement with other parametrization of δ_{33}. We also encounter the well-known problem[50] that $g_{\pi N\Delta}$ and M_Δ are mildly sensitive to the form of parametrization of δ_{33}.

In Olsson's method we use a trick first developed by him.[18] We have

$$\tan\delta_{33}=\frac{1+\epsilon\tan\delta_B}{\epsilon+\tan\delta_B}\ . \tag{25}$$

Now setting $\tan\delta_{33}=\pm1$ and solving for ϵ, we get

$$\epsilon(\tan\delta_{33}=\pm1)=\pm1\ . \tag{26}$$

We thus have two equations from which we may solve for the unknowns $g_{\pi N\Delta}$ and M_Δ. Using the phase shifts listed by Berends and Donnachie,[22] we find $g_{\pi N\Delta}=1.935$ and $M_\Delta=1216.53$ MeV. With $g_{\pi N\Delta}$ and M_Δ now known, we can use Eq. (25) to solve for δ_B.

In the K-matrix approach, we treat the tree-level amplitudes as K-matrix elements and obtain

$$\tan\delta_{33}=qf_{1+}^{B}+qf_{1+}^{R}=\tan\delta_B+\frac{M_\Delta\Gamma_\Delta(s)}{M_\Delta^2-s}\ . \tag{27}$$

In this approach, the mass of the Δ is the energy at which δ_{33} passes through 90°. The coupling constant $g_{\pi N\Delta}$ may be determined by the residue of the K matrix pole.[29] From the phase shifts given by Berends and Donnachie (BD), we obtain $M_\Delta=1232.49$ and $g_{\pi N\Delta}=2.15$ It is also useful to assume some functional form for $\tan\delta_B$ and fit the δ_{33} phase shift throughout the Δ region. This will allow us to look for form-factor effects and also give an idea of how good this unitarization method is. In particular, we assume

$$\tan\delta_B=a\left[\frac{q}{m}\right]^3+b\left[\frac{q}{m}\right]^5\ , \tag{28}$$

and fit a, b, M_Δ, and $g_{\pi N\Delta}$ to δ_{33}. The form of (28) is chosen to give the correct threshold dependence q^3 plus the additional free term q^5. We obtain $a=0.100$, $b=-0.012$, $M_\Delta=1231.65$ MeV, and $g_{\pi N\Delta}=2.164$, with a χ^2 per degree of freedom of 0.45. Since the errors on δ_{33} are not given by BD, we have assumed conservatively an error of 1 degree at every energy. The background phase shift δ_B is in good agreement with the theoretical prediction of δ_B obtained by Olsson.[18] If we allow some energy dependence of $g_{\pi N\Delta}$ of the form (which is valid for W in the neighborhood of M_Δ)

$$g_{\pi N\Delta}(s)=g_{\pi N\Delta}(M_\Delta^2)+\frac{B(s-M_\Delta^2)}{M_\Delta^2}+\frac{C(s-M_\Delta^2)^2}{M_\Delta^4}\ , \tag{29}$$

we find $B\approx0$, $C\approx-1.47$, but the χ^2 per degree of freedom actually increases to 0.46. This amounts to a variation in $g_{\pi N\Delta}$ (in the s channel) of about 10% over the energy range considered here.

In Noelle's method,

$$\delta_{33}=\delta_R+\delta_B\ , \tag{30}$$

where we assume δ_B is given by (28) and

$$\tan\delta_R=\frac{M_\Delta\Gamma_\Delta(s)}{M_\Delta^2-s}\ , \tag{31}$$

with $\Gamma_\Delta(s)$ given by (22). We again fit the parameters to the δ_{33} phase shift and obtain $a=0.084$, $b=-0.0096$, $M_\Delta=1250.13$ MeV, and $g_{\pi N\Delta}=2.4604$ with a χ^2 per degree of freedom of 0.45.

It is interesting to note that for both the Olsson and K-matrix methods we could find energies at which we can determine M_Δ and $g_{\pi N\Delta}$ independently of what is *defined* to be background in that model. This is also true for Noelle's method. Recall that the partial wave $f_{1+}^{3/2}$ has a pole in the complex W plane when $\cot\delta_{33}=i$. Thus, in Noelle's method,

$$\tan\delta_{33}=\frac{\tan\delta_R+\tan\delta_B}{1-\tan\delta_R\tan\delta_B}=-i\ , \tag{32}$$

where all phases are evaluated at the T-matrix pole position. This implies

$$(1-i\tan\delta_B)(1-i\tan\delta_R)=0\ . \tag{33}$$

This gives $\tan\delta_R=-i$ provided $\tan\delta_B\neq-i$. At the T-matrix pole position, $W\approx(1210-50i)$ MeV,[31] and assuming we can extrapolate (28) into the complex W plane, we obtain $\tan\delta_B\approx(0.20-0.12i)$ at the pole position, implying that $\tan\delta_R=-i$ at the pole. We thus find from the T-matrix pole position[31] $g_{\pi N\Delta}=2.53$ and $M_\Delta=1254$ MeV, in good agreement with the values obtained in the fit.

In summary, $g_{\pi N\Delta}$ and M_Δ are determined by the energies at which $\tan\delta_{33}=\pm1,\infty,-i$, for the Olsson, K-matrix, and Noelle methods, respectively.

It is interesting to compare the above three unitarization methods for πN scattering in an expansion and associate the terms in the expansion with terms in a perturbation series. To illustrate the usefulness of this approach, first consider the case where f_B is zero, and iterate f_R ignoring the dispersive corrections

$$qf_{1+}=f_R[1+if_R+(if_R)^2+\cdots]=\frac{f_R}{1-if_R}\ , \quad (34)$$

the final expression being valid for any value of f_R. We see that with $f_B=0$, this is precisely what all three unitarization methods for T yield. For an arbitrary background,

$$T\equiv qf_{1+}=\frac{\tan\delta}{1-i\tan\delta}=\frac{f_R+f_B}{1+\eta f_R f_B-i(f_R+f_B)}\ , \quad (35)$$

which we formally expand

$$T=(f_R+f_B)\left[1+\sum_{n=1}^{\infty}[i(f_R+f_B)-\eta f_R f_B]^n\right]\ . \quad (36)$$

For simplicity, consider the terms up to $f_R^p f_B^q$ with $p+q=3$:

$$T\approx(f_R+f_B)[1+i(f_R+f_B)-\eta f_R f_B -(f_R^2+2f_R f_B+f_B^2)]\ , \quad (37)$$

or

$$T\approx f_R+f_B+i(f_R^2+2f_R f_B+f_B^2)-f_R^3-f_B^3 -(3+\eta)(f_R^2 f_B+f_R f_B^2)\ . \quad (38)$$

Thus, the three methods discussed earlier disagree on the contribution of the $f_R^2 f_B$ and $f_R f_B^2$ terms. In the approximation of ignoring dispersive corrections, assuming separability, and summing an infinite subset of unitary diagrams, we would have for the $f_R^2 f_B$ terms the diagrams of Fig. 1, indicating that the coefficient of the $f_R^2 f_B$ should be -3 as given by the *K-matrix* (the minus sign arises from the phase i obtained from each of the intermediate propagators when evaluated on shell). To this order, and also to higher orders, Noelle's method "undercounts" the number of diagrams (i.e., the coefficient of the background-resonance interference term is smaller than what one obtains based on the above arguments) and Olsson's method "overcounts" the number of diagrams.

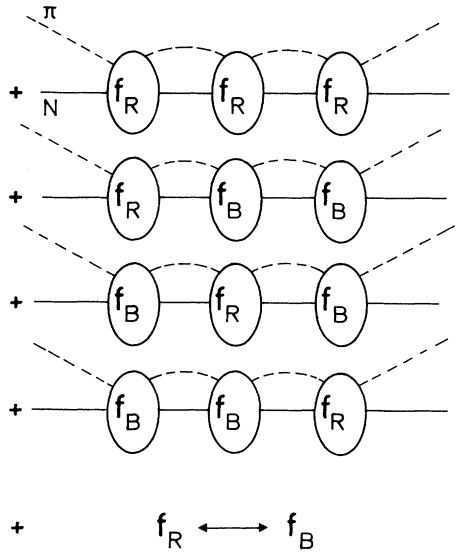

FIG. 1. Diagrams of the form $f_R^p f_B^q$ with $p+q=3$ (see text).

E. Unitarity for photoproduction of pions

The tree approximation for the $M_{1+}^{3/2}$ and $E_{1+}^{3/2}$ pion-photoproduction multipoles takes the form

$$A=A_B+\frac{N}{\epsilon}\ , \quad (39)$$

where, for the $M_{1+}^{3/2}$ multipole,

$$N_M=\frac{eS_1 km}{4g_{\pi N\Delta}S_2 q^2 M(W+M)} \times\left[g_{1\Delta}(3W+M)-\frac{g_{2\Delta}W(W-M)}{2M}\right]\ , \quad (40)$$

and, for the $E_{1+}^{3/2}$ multipole,

$$N_E=\frac{-eS_1 km(W-M)}{4g_{\pi N\Delta}S_2 q^2 M(W+M)}\left[g_{1\Delta}-\frac{g_{2\Delta}W}{2M}\right]\ , \quad (41)$$

with $S_{1(2)}=\sqrt{E_{i(f)}+M_{i(f)}}$, i and f being the incoming and outgoing nucleon, respectively, and ϵ is given by (21). A_B is the projection of the nonresonant contribution in these multipoles. We may also *define*

$$(R_{\rm EM})=\frac{-(W-M)}{3W+M}\left[\frac{g_{1\Delta}-g_{2\Delta}\frac{W}{2M}}{g_{1\Delta}-g_{2\Delta}\frac{W(W-M)}{2M(3W+M)}}\right]\ . \quad (42)$$

When $W=M_\Delta$, this agrees with expressions (2) and (3), and the results we give are for $(R_{\rm EM})_{M_\Delta}$ with M_Δ given by the appropriate unitarization procedure. We will also give results for $\tilde{W}$, the energy at which $R_{\rm EM}=0$, to show that in most fits $\tilde{W}>1500$ MeV.

In Olsson's approach, the pion-photoproduction amplitude in the resonant channels is unitarized in the following manner. The background is assumed to be separately unitary and, thus,

$$A_B\rightarrow A_B e^{i\delta_B}\ , \quad (43)$$

where δ_B is calculated from (25) by taking the δ_{33} as input. We note that A_B includes all contributions to the resonant multipoles except the s-channel Δ exchange. In particular, A_B has contributions from the u-channel Δ exchange. Thus, $A_B=A_B(g_{1\Delta},g_{2\Delta},X,Y,Z)$, the arguments of A_B being in parentheses.

The resonant piece is modified by

$$\frac{N}{\epsilon}\rightarrow\frac{Ne^{i\phi}}{\epsilon-i\gamma}\ , \quad (44)$$

where

$$\frac{1}{\epsilon-i\gamma}=\sin(\delta-\delta_B)e^{i(\delta+\delta_B)}\ . \quad (45)$$

The phase ϕ is determined from Watson's[45] theorem:

$$A = A_B e^{i\delta_B} + \frac{Ne^{i\phi}}{\epsilon - i\gamma} = |A| e^{i\delta} . \tag{46}$$

The solution for ϕ is

$$\phi = \delta_p + \delta_B , \tag{47}$$

where

$$\sin\delta_p \equiv \frac{A_B}{N} . \tag{48}$$

The resonant multipoles finally take the form

$$A = N \sin(\delta - \delta_B + \delta_p) e^{i\delta} . \tag{49}$$

This method fails if $|A_B| > |N|$, which can happen for the $E_{1+}^{3/2}$ multipole. For our case, we overcome this problem by applying Olsson's method directly to the helicity amplitudes[4] rather than to the multipoles, with the helicity amplitudes defined by

$$A_{1+} = \tfrac{1}{2}(3E_{1+} + M_{1+}) , \tag{50}$$

$$B_{1+} = \frac{\sqrt{3}}{2}(E_{1+} - M_{1+}) . \tag{51}$$

There is nothing unique about unitarizing the helicity amplitudes. We could have chosen some other combination of $E_{1+}^{3/2}$ and $M_{1+}^{3/2}$ to unitarize as long as each is $M_{1+}^{3/2}$ dominated and the transformation is orthogonal.

In Noelle's method, the final form of the resonant multipoles is

$$A = (A_B \cos\delta + N \sin\delta_R) e^{i\delta} . \tag{52}$$

This unitarization method works for any ratio A_B/N and has recently been used by Cenni, Dillon, and Christillin.[51]

Treating the tree-level amplitudes as K-matrix elements, we obtain

$$A = \cos\delta e^{i\delta} \left(A_B + \frac{N}{\epsilon} \right) . \tag{53}$$

This is not the best form of the amplitude for fitting the data because one must make sure that $\cos\delta$ and ϵ go to zero, with $\cos\delta/\epsilon$ finite, at the same energy. Recalling that in the K-matrix approach

$$\tan\delta = \tan\delta_B + \frac{1}{\epsilon} , \tag{54}$$

Eq. (53) may be recast in the form

$$A = \frac{\sin\delta e^{i\delta}}{1 + \epsilon \tan\delta_B} (\epsilon A_B + N) . \tag{55}$$

This is the best form of fitting the data and also works for any values of N and A_B.

The different unitarization procedures differ on how to incorporate the πN final-state rescattering. If there is no background contribution so that $\tan\delta_B = A_B = 0$, then all three methods trivially agree and give

$$A = N \sin\delta e^{i\delta} . \tag{56}$$

However, the background *is* important, especially for the $E_{1+}^{3/2}$ multipole. The importance of the background for πN scattering can be seen by comparing various values of M_Δ and $g_{\pi N\Delta}$ obtained in the various approaches. However, even if $\tan\delta_B = 0$, and all three methods are identical in *form,* it is not guaranteed that all methods will give the same M_Δ and $g_{\pi N\Delta}$ since the (model-dependent) width is being evaluated at different energies. Finally we note that for all methods, $\delta_B \approx 15°$ near resonance.

III. RESULTS

The amplitude has been cast in a (model-dependent) unitary form and $g_{1\Delta}$, $g_{2\Delta}$, X, Y, and Z may be fitted to the pion-photoproduction data. We choose to fit the multipoles rather than the observables (cross section, polarizations, etc.) for the following reasons. First, all the observables may be expressed in terms of the multipoles, and thus if the extracted multipoles are a good representation of the observables, and our model gives a good fit to the multipoles, then our model should also be in good agreement with the observables. We show below that our model is in good agreement with the observables. Second, the resonant piece of the Δ contributes only to the $E_{1+}^{3/2}$ and $M_{1+}^{3/2}$ multipoles. How well the background in these multipoles is known can be gauged by how well the model reproduces the nonresonant multipoles. Third, deficiencies in the model may be more apparent when comparing with the multipoles than when comparing with the observables. For example, the failure to reproduce the $M_{1-}^{1/2}$ multipole *might* indicate the importance of inelasticities in the P_{11} phase shift.

In the first resonance region, very few theoretical assumptions are needed for the energy-independent multipole analyses, but in many cases the different multipole sets are *not* in good mutual agreement, reflecting the difficulties in extracting multipoles from the cross section and polarizations. Since it is not clear which of the extant multipole sets is the best, we give our results for various sets available in the literature. This gives us some estimate on the errors arising due to the imprecision of the multipole data base. For most data sets, we have performed fits to the full energy range, and also to a truncated energy range around $W \approx M_\Delta$. This procedure allows us to test the need for form factors, particularly at the Δ vertices. The fits to the data have been done with all three unitarization procedures and with different ωNN couplings. We also compare the K-matrix parameters predicted by the various fits with those extracted model independently from the data.

When investigating the effect of theoretical uncertainties, for example, the uncertainties in the ωNN couplings, on the extracted $E2$ and $M1$ amplitudes, we have used the data of BD and to a lesser extent the data of PS. This is because these data sets have been fully isospin decomposed, and the data of BD are available every 10 MeV from a photon laboratory energy of 240 to 450 MeV. Finally, for the data sets that have used only the γp data, and thus are not fully isospin decomposed, we have included ρ exchange with $g_{\rho 1} = 2.66$, $g_{\rho 2} = 16.23$, and $M_\rho = 770.3$ MeV. This choice of $g_{\rho 1}$ and $g_{\rho 2}$ gives a good

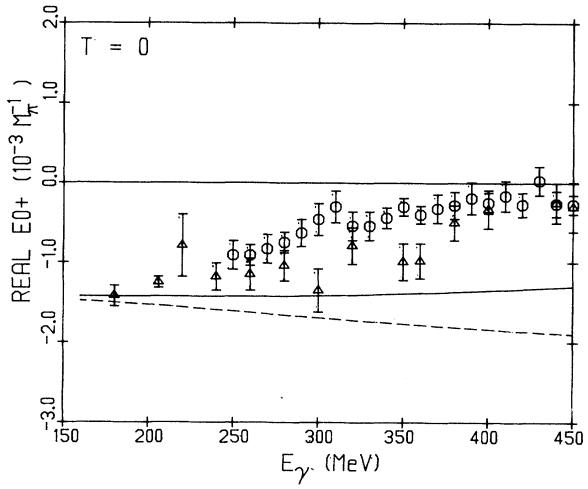

FIG. 2. The real part of E^0_{0+} in units of $10^{-3}M_\pi^{-1}$ vs photon laboratory energy, E_γ. The dashed line is the PV nucleon Born contribution and the solid line is PV nucleon Born plus ρ exchange. The data are from Berends and Donnachie (circles) and Pfeil and Schwela (triangles). The parameters used are those of Table I(a), row 1.

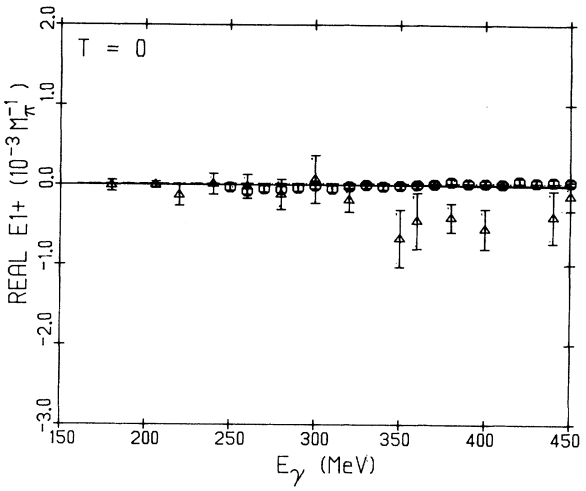

FIG. 4. Real part of E^0_{1+}. Curves and data same as in Fig. 2.

fit to the $T=0$ multipoles (see Figs. 2–5).

Tables I(a) and I(b) give the results from the various fits to the full energy region. The data sets are indicated by the initials of the authors whose data have been fitted: Berends and Donnachie[22] (BD), Pfeil and Schwela[23] (PS), Grushin *et al.*[25] (GRU), Get'man *et al.*[14] (GET), and Miroshnichenko *et al.*[26] (MIR). The column "unit" contains an abbreviation for the unitarization procedure used in the fit: Olsson (OL), K matrix (K), and Noelle (N). The resulting values for $g_{1\Delta}$, $g_{2\Delta}$, X, Y, and Z are given along with the χ^2 per degree of freedom, $\chi^2_{\rm DF}$. To give an idea of the quality of our fits to the experimentally extracted resonant multipoles, we also have included χ^2_{ME}, which is defined as the sum of the χ^2 for the $E^{3/2}_{1+}$ and $M^{3/2}_{1+}$ multipoles divided by $2(N-1)$, N being the number of data points fit in each multipole. We also give χ^2_B which is the sum of the χ^2 from the nonresonant multipoles divided by $8N-5$. Finally, we include the global averages for our fitted quantities, AVG, as well as averages restricted to a given unitarization method, AVG U, to illustrate the model dependence in the extraction of the parameters.

Tables II(a) and II(b) give the values for the $N\leftrightarrow\Delta$ electromagnetic transition amplitudes, as defined in Eqs. (2) and (3), resulting from $g_{1\Delta}$ and $g_{2\Delta}$ given in Table I. $E2$, $M1$, $A_{1/2}$, and $A_{3/2}$ are all in the standard units of 10^{-3} $\mathrm{GeV}^{-1/2}$, and the $E2$-to-$M1$ ratio (EMR) is given in percent. We have also included, in units of MeV, the energy $\tilde{W}$ at which $R_{\rm EM}$ becomes zero. For all entries in this table, we have used the mass of the Δ appropriate to the unitarization method used in the fit.

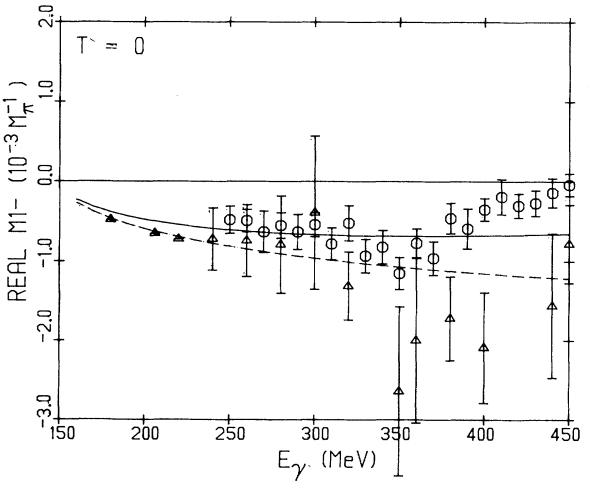

FIG. 3. Real part of M^0_{1-}. Curves and data same as in Fig. 2.

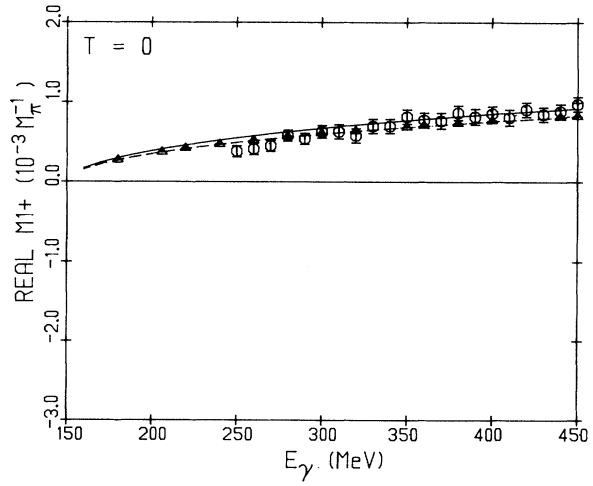

FIG. 5. Real part of M^0_{1+}. Curves and data same as in Fig. 2.

TABLE I. (a) Results for the $\gamma N\Delta$ gauge couplings $g_{1\Delta}$ and $g_{2\Delta}$, and the off-shell parameters X, Y, and Z obtained from different fits with $g_{\omega 1}=-g_{\omega 2}=7.98$. Also given are the total χ^2 per degree of freedom, $\chi^2_{\rm DF}$, the χ^2 from the resonant multipoles, χ^2_{ME} and the χ^2 from the background multipoles, χ^2_B. The overall average is given along with the averages for a fixed unitarization method. SD is the standard deviation calculated with $N-1$ weighting. GET10 and GRU6 have been excluded in the global average for Z. Including these values gives $Z=1.37\pm6.05$. (b) Results for gauge couplings and off-shell parameters obtained for different values of $g_{\omega 1}$ and $g_{\omega 2}$. The first number below the data set being fitted is $g_{\omega 1}$ and the second number is $g_{\omega 2}$. The notation is as in (a).

Data	Unit	$g_{1\Delta}$	$g_{2\Delta}$	Z	Y	X	$\chi^2_{\rm DF}$	χ^2_{ME}	χ^2_B
					(a)				
BD22	OL	4.56	5.49	−0.24	−0.53	2.39	14.2	4.74	13.0
BD22	*K*	5.00	5.18	−0.27	−0.89	3.81	29.7	59.3	15.1
BD22	N	5.79	3.34	−0.28	−1.24	9.25	77.2	21.6	24.1
PS11	OL	4.74	6.00	−0.38	−0.65	2.81	5.04	6.95	3.37
PS11	*K*	5.15	6.30	−0.40	−0.66	2.87	27.5	101	3.16
PS11	N	5.83	6.54	−0.49	−0.34	2.95	69.8	272	4.25
GET10	OL	4.66	5.34	+1.26	−0.25	0.03	84.5	298	13.0
GET10	*K*	5.05	5.54	−0.20	+0.17	−0.18	27.3	46.4	16.2
GET10	N	5.79	5.58	−0.22	−0.04	0.49	431	411	32.4
MIR11	OL	4.06	4.34	−0.22	+1.20	−2.81	1453	5971	14.2
MIR11	*K*	4.65	5.55	−0.19	+0.47	−1.05	1000	4077	17.6
MIR11	N	5.25	5.52	−0.15	+0.10	−0.30	1424	5768	34.1
GRU6	OL	4.82	5.04	+23.2	−0.31	−0.35	5.13	2.19	4.62
GRU6	*K*	5.22	5.97	−0.45	−1.01	4.23	33.6	1.53	33.2
GRU6	N	5.93	6.39	−0.43	−0.84	4.29	31.6	2.75	31.0
AVG		5.10	5.47	−0.30	−0.32	1.90			
SD		0.55	0.82	0.11	0.63	2.96			
AVG U	OL	4.57	5.24	4.72	−0.11	0.41			
SD		0.30	0.61	10.35	0.75	2.28			
AVG U	*K*	5.01	5.71	−0.30	−0.38	1.94			
SD		0.22	0.43	0.12	0.66	2.40			
AVG U	N	5.72	5.47	−0.31	−0.47	3.34			
SD		0.27	1.28	0.14	0.56	3.79			
					(b)				
BD22 14,0	OL	4.52	4.40	+0.69	−0.40	0.73	32.0	7.60	30.1
BD22 0,0	OL	4.60	7.21	+0.10	−0.10	0.23	11.6	15.5	7.8
BD22 8,0	OL	4.55	5.59	+0.39	−0.33	0.56	17.6	5.2	16.3
BD22 3.46, −23.2	OL	4.59	6.23	−0.53	−0.42	4.31	8.50	5.60	7.12
BD22 8,−8	OL	4.29	0.00 fixed	−0.31	0.74		28.1	47	16.5
BD22 8,0	*K*	5.00	5.43	−0.04	−0.39	1.23	32.7	57	18.7
BD22 0,0	*K*	5.07	7.05	−0.10	−0.04	0.21	21.2	53	8.16
BD22 8,0	N	5.72	3.97	−0.23	−0.73	4.53	78.7	209	27.4
BD22 0,0	N	5.82	6.24	−0.19	−0.06	0.57	62.3	189	16.0
GET10 8,0	OL	4.66	5.49	8.25	−0.31	−0.28	87.4	305	14.2

Table III contains the results of the fits to the truncated energy region for $g_{1\Delta}$, $g_{2\Delta}$, X, Y, and Z. The notation is the same as in Table I. For the truncated fits, we have restricted the fits to the following energy regions; BD, $320 \leq k_l \leq 380$ (7 points); PS, $300 \leq k_l \leq 380$ (5 points); GET, $300 \leq k_l \leq 380$ (5 points); and MIR, $300 \leq k_l \leq 380$ (5 points), where k_l is the photon laboratory energy in MeV. We did not perform a truncated fit for GRU since the data set is already limited to six energies around the Δ mass. Table IV is analogous to Table II, but contains the electromagnetic amplitudes resulting from the truncated fits.

We have fitted all the $T=\frac{1}{2}$ and $T=\frac{3}{2}$ multipoles with $l \leq 1$, l being the pion-nucleon orbital angular momentum. The minimization has been performed by the CERN routine MINUIT with the function

TABLE II. (a) Transition amplitudes resulting from the fits listed in Table I(a) in units of 10^{-3} $\mathrm{GeV}^{-1/2}$. Also given are the EMR (in percent) and the energy $\tilde{W}$ (in MeV) at which R_{EM} becomes zero. (b) Transition amplitudes resulting from the fits in Table I(b).

Data	Unit	$E2$	M1	$A_{1/2}$	$A_{3/2}$	EMR (%)	$\tilde{W}$
				(a)			
BD22	OL	−3.47	249	−119	−218	−1.39	1590
BD22	*K*	−5.98	282	−132	−249	−2.12	1780
BD22	N	−14.3	343	−150	−309	−4.18	3240
PS11	OL	−2.96	258	−125	−226	−1.15	1490
PS11	*K*	−3.78	288	−138	−253	−1.31	1540
PS11	N	−5.97	337	−159	−297	−1.77	1680
GET10	OL	−4.14	255	−121	−224	−1.63	1640
GET10	*K*	−5.25	284	−134	−251	−1.86	1710
GET10	N	−8.36	337	−156	−299	−2.48	1950
MIR11	OL	−4.34	223	−105	−197	−1.95	1760
MIR11	*K*	−3.75	266	−125	−299	−1.44	1570
MIR11	N	−6.34	304	−143	−269	−2.09	1790
GRU6	OL	−5.36	264	−124	−234	−2.03	1800
GRU6	*K*	−4.85	293	−139	−258	−1.66	1640
GRU6	N	−6.75	343	−161	−303	−1.97	1740
AVG		−5.71	288	−135	−254	−1.94	
SD		2.78	38	16	35	0.71	
AVG	OL	−4.05	250	−119	−220	−1.63	
SD		0.91	16	8	14	0.37	
AVG U	*K*	−4.72	283	−134	−248	−1.68	
SD		0.96	10	6	11	0.32	
AVG U	N	−8.34	333	−154	−295	−2.50	
SD		3.45	16	7	15	0.98	
				(b)			
BD22 14,0	OL	−5.79	249	−116	−221	−2.33	1930
BD22 0,0	OL	+0.30	247	−124	−214	+0.10	1200
BD22 8,0	OL	−3.22	248	−119	−218	−1.30	1530
BD22 3.46 −23.2	OL	−1.93	249	−122	−217	−0.77	1380
BD22 8,−8	OL	−14.9	247	−101	−223	−6.05	always neg.
BD22 8,0	*K*	−5.36	281	−133	−248	−1.90	1730
BD22 0,0	*K*	−1.63	282	−138	−245	−0.58	1350
BD22 8,0	N	−12.4	337	−150	−303	−3.68	2710
BD22 0,0	N	−6.71	337	−158	−298	−1.99	1750
GET10 8,0	OL	−3.82	254	−121	−224	−1.50	1750

TABLE III. Results for the truncated fits. Notation same as Table I(a). The precise energy region used in the truncated fits is given in the text.

Data	Unit	$g_{1\Delta}$	$g_{2\Delta}$	Z	Y	X	χ^2_{DF}	χ^2_{ME}	χ^2_B
BD7	OL	4.64	6.73	−0.13	−0.42	1.58	8.30	0.98	8.07
BD7	K	5.11	6.97	−0.23	−0.72	2.47	50.3	177	8.65
BD7	N	5.83	6.99	−0.27	−1.08	3.94	163	630	14.8
PS5	OL	4.73	6.36	−0.26	1.82	−4.19	2.60	3.10	1.89
PS5	K	5.03	6.51	−5.38	−0.34	−0.50	48.0	199	2.51
PS5	N	5.63	7.09	−0.15	−0.20	−0.34	109	463	3.17
GET5	OL	4.67	5.66	7.49	−0.30	−0.25	157	603	19.2
GET5	K	5.02	5.87	−0.25	0.86	−1.71	22.0	21.0	17.2
GET5	N	5.74	6.37	−0.21	0.26	−0.30	154	541	30.3
MIR5	OL	3.97	5.34	−0.46	−1.38	5.32	3243	13 992	44.8
MIR5	K	4.56	5.86	6.70	−0.31	−0.29	2169	9 318	39.2
MIR5	N	5.14	6.26	−0.22	1.44	−3.88	4169	12 852	1231
AVG		5.01	6.33	0.55	−0.03	0.15			
SD		0.54	0.56	3.40	0.97	2.83			
AVG U	OL	4.50	6.02	1.66	−0.07	0.62			
SD		0.36	0.64	3.89	1.35	3.95			
AVG U	K	4.93	6.30	0.21	−0.13	−0.01			
SD		0.25	0.54	4.96	0.68	1.77			
AVG U	N	5.59	6.68	−0.21	0.11	−0.15			
SD		0.31	0.42	0.05	1.05	3.20			

$$\chi^2=\sum_{i=1}^{8}\sum_{W=W_{\min}}^{W_{\max}}\frac{[\mathrm{Re}M_i^e(W)-\mathrm{Re}M_i^T(g_{1\Delta},g_{2\Delta},X,Y,Z)]^2}{\sigma_i^2(W)} \tag{57}$$

being minimized. Here, $\mathrm{Re}M_i^e(W)$ is the real part of the ith experimental multipole at energy W, σ_i is the experimental error and M_i^T is the prediction of M_i^e. Although the χ^2 has many local minima, we have found that the final parameters given by MINUIT do not depend on the starting parameters for the present problem. Finally, the errors on parameters given by MINUIT are generally much smaller than the errors given in Tables I and III. The averages and errors (denoted by SD) in these tables are simply the usual average and standard deviation (with $N-1$ weighting) of the appropriate parameters.

TABLE IV. Transition amplitudes for the truncated fits. Notation same as Table II(a).

Data	Unit	$E2$	$M1$	$A_{1/2}$	$A_{3/2}$	EMR (%)	$\tilde{W}$
BD7	OL	−0.97	251	−124	−218	−0.39	1300
BD7	K	−1.99	284	−139	−248	−0.70	1380
BD7	N	−4.76	336	−161	−295	−1.42	1570
PS5	OL	−2.12	257	−125	−224	−0.83	1400
PS5	K	−2.82	281	−136	−246	−1.01	1450
PS5	N	−3.67	323	−156	−283	−1.14	1490
GET5	OL	−3.49	255	−122	−224	−1.37	1550
GET5	K	−4.37	282	−134	−248	−1.55	1610
GET5	N	−6.04	332	−157	−292	−1.82	1690
MIR5	OL	−1.77	215	−105	−188	−0.82	1400
MIR5	K	−2.67	254	−123	−223	−1.05	1460
MIR5	N	−3.89	295	−142	−259	−1.32	1540
AVG		−3.21	280	−135	−246	−1.12	
SD		1.44	37	17	33	0.40	
AVG U	OL	−2.09	245	−119	−214	−0.85	
SD		1.05	20	9	17	0.40	
AVG U	K	−2.96	275	−133	−241	−1.08	
SD		1.01	14	7	12	0.35	
AVG U	N	−4.59	322	−154	−282	−1.43	
SD		1.08	18	8	16	0.29	

IV. DISCUSSION

We start this section with a few remarks on the fitting of the multipole data sets. As remarked earlier, the advantage to fitting the multipoles is that small dynamical effects in the amplitude are more visible, provided that the multipoles themselves are reliably extracted. To give some examples, we find that the parameters X, Y, and Z are determined by very specific multipoles. We can clearly see the u-channel Δ effect in certain multipoles. Finally, by examining the $E_{1+}^{3/2}$ multipole we can gain information on the nonvanishing value of the resonant $E2$ amplitude. Of course, all this information is buried in the observables, the multipole decomposition nicely sorts this out.

The largest disadvantage to fitting the multipoles is that the different multipole sets are in poor agreement if we believe the given errors. Table V is a comparison of the $M_{1+}^{3/2}$ multipole as given by BD, MIR, and GET at energies common to all sets. We have combined the data sets to obtain the (weighted) average multipole and error, and then have calculated the scaling factor, s (not to be confused with the square of the c.m. energy), as defined by the Particle Data Group[31] (PDG). Since $s>1$ indicates inconsistent data, we conclude that only at the first energy are the sets in agreement, and the discrepancies

TABLE V. A comparison of the $M_{1+}^{3/2}$ multipole at various photon laboratory energies, E_γ, as given by Berends and Donnachie, Miroshnichenko *et al.*, and Get'man *et al.* The weighted average is given along with the scaling factor, *s*.

E_γ	BD	MIR	GET	AVG	S
250	23.2 ±0.3	23.28 ±0.20	23.18±0.28	23.24±0.14	0.23
280	26.1 ±0.2	26.43 ±0.07	25.92±0.08	26.20±0.05	3.41
300	20.8 ±0.1	22.78 ±0.05	21.24±0.04	21.75±0.03	18.4
320	9.84±0.04	13.94 ±0.02	11.08±0.02	12.21±0.01	84.2
350	−4.33±0.02	−2.307±0.004	−4.43±0.01	−2.66±0.004	152
360	−8.93±0.04	−6.32 ±0.01	−7.66±0.03	−6.59±0.01	52.1
380	−12.2 ±0.1	−10.73 ±0.03	−11.66±0.03	−11.24±0.02	21.7
400	−13.2 ±0.1	−12.81 ±0.04	−13.22±0.05	−12.99±0.03	4.79
420	−13.2 ±0.1	−13.20 ±0.07	−13.55±0.08	−13.32±0.05	2.51
450	−11.8 ±0.2	−12.43 ±0.12	−13.24±0.11	−12.72±0.08	4.97

are largest around the resonance energy of $E_\gamma \approx 340$ MeV. Although this table illustrates the worst cases, we conclude that the errors on the multipoles have been generally underestimated. As a consequence, we do not know if any statistical significance should be attached to the χ^2 in Table I, but the χ^2 are still useful when comparing *different* fits to the *same* data set. We hope the discrepancies amongst the multipole data sets can be resolved by future experimental research at the emerging facilities.

A. X, Y, Z

In an analysis of BD's data, Olsson and Osypowski found $Z=-0.29\pm0.10$ and $Y=0.78\pm0.30$ with $g_{\omega 1}=7.98$ and $g_{\omega 2}=-6.46$. With $g_{\omega 1}=-g_{\omega 2}=7.98$ and $g_{2\Delta}=0$, we find that the best fit to BD's data is obtained with $Z=-0.31$ and $Y=0.74$. With arbitrary $g_{2\Delta}$, we obtain the best fit with $Z=-0.24$, $Y=-0.53$, and $X=2.39$, but these values are very sensitive to the values of $g_{\omega 1}$ and $g_{\omega 2}$. For example, with $g_{\omega 1}=g_{\omega 2}=0$, the best fit occurs for $Z=0.10$, $Y=-0.10$, and $X=0.23$, and the χ^2 is reduced by about 20%. On the other hand, χ^2_{ME} increases by a factor of 3. We should recall that Olsson and Osypowski[48] found $Z=-0.45\pm0.20$ in an analysis of πN scattering.

The off-shell parameters are also very sensitive to the data set being fitted, and in some cases the off-shell parameters show a large dependence on the unitarization method. In particular, fitting the data of GET and GRU with Olsson's method gives $Z=1.26$ and 23.2, respectively. On the other hand, fitting the same data with K or N gives $-0.43 \lesssim Z \lesssim -0.22$. There are also large correlations (as given by MINUIT) amongst the off-shell parameters, but $g_{1\Delta}$ and $g_{2\Delta}$ are only slightly correlated with the off-shell parameters. They are, however, correlated with each other. The correlation between $g_{1\Delta}$ and $g_{2\Delta}$ arises because the $M_{1+}^{3/2}$, having relatively small errors compared to the $E_{1+}^{3/2}$, essentially fixes the linear combination of $g_{1\Delta}$ and $g_{2\Delta}$ appearing in Eq. (40) with $W \approx M_\Delta$, i.e., the $M_{1+}^{3/2}$ multipole essentially determines

$$g_{1\Delta}(3M_\Delta+M)-g_{2\Delta}\frac{M_\Delta(M_\Delta-M)}{2M} .$$

Despite the large uncertainties in the off-shell parameters, it is useful to compare our results with the parameter choices of Nath and Bhattacharyya[19] and Peccei.[12,46] The value $g_{2\Delta}=0$ is ruled out not only by the $E_{1+}^{3/2}$, but also by the $E_{0+}^{1/2}$ and $E_{0+}^{3/2}$ multipoles. Figures 6 and 7 show the large $g_{2\Delta}$ contribution to these two nonresonant multipoles. The contribution to the $E_{0+}^{1/2}$ is due solely to the u-channel Δ exchange, whereas the Δ contribution to the $E_{0+}^{3/2}$ multipole contains both s- and u-channel contributions. Although all fits rule out $g_{2\Delta}=0$, the status of Z and Y is less certain. In none of our fits do Nath's values arise, and setting $Z=0.5$, $Y=0$ generally results in a large increase in the χ^2. For many fits Z is close to -0.25, but Y and X generally differ widely from -0.25. Most fits give $|Z| \lesssim 0.5$, but there are large exceptions. As discussed by Nath, Etemadi, and Kimel,[39] there seems to be no firm basis for Peccei's choice of the off-shell parameters, and as we have discussed here and elsewhere,[34] Nath's choice of the off-shell parameters and particularly

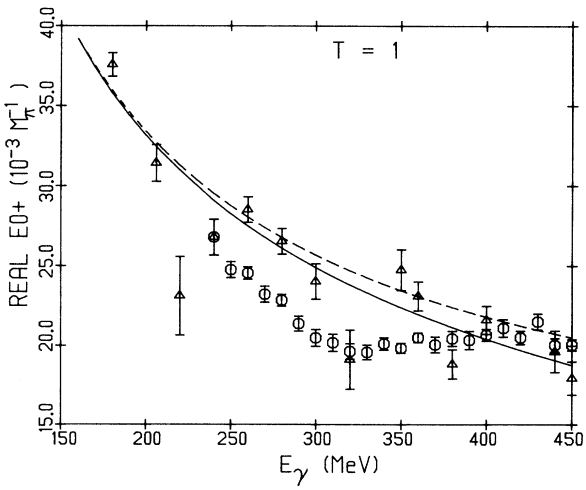

FIG. 6. Real part of $E_{0+}^{1/2}$. The dashed line is the PV nucleon Born and the solid line is the total contribution including ω and Δ exchanges. The ω contribution is negligible here. Data as in Fig. 2.

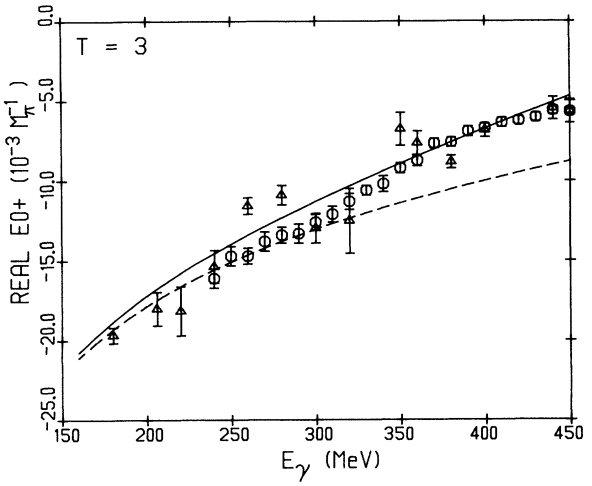

FIG. 7. Real part of $E_{0+}^{3/2}$. Curves and data same as in Fig. 6.

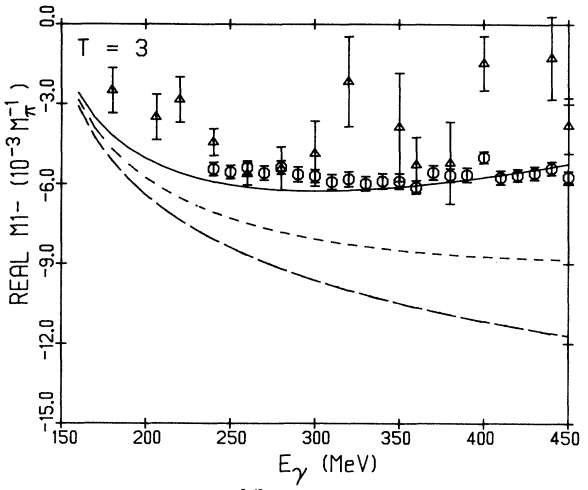

FIG. 9. Real part of $M_{1-}^{3/2}$. Curves and data same as Fig. 8, except $P_{11}(1440)$ contribution not shown.

$g_{2\Delta}$ seem to be too restrictive for a phenomenological description of transitions between composite particles. Unfortunately we do not know how to predict these parameters starting from a composite model of hadrons.

Regardless of the values of the off-shell parameters, we find that Z is determined largely by the $M_{1-}^{3/2}$ multipole, Y by the $M_{1+}^{1/2}$, and X by $E_{0+}^{1/2,3/2}$. The other multipoles are largely insensitive to the off-shell parameters. What we mean by this can be illustrated by an example: if we vary Z keeping all other parameters fixed, it is the $M_{1-}^{3/2}$ multipole that is affected the most.

B. Background multipoles

Before turning to the resonant multipoles, we must mention one concern, which is the lack of form factors, particularly at the ω and Δ vertices. In the s channel, the Δ is close to being on shell ($W \approx M_\Delta$) throughout the energy region we are fitting, and thus the lack of a form factor is justified. However, in the u channel, $(u-M_\Delta^2)/M_\Delta^2 \approx -0.7$, indicating that the Δ is far off shell. Given the quality of data and our general agreement with the data (see Figs. 6–13), we see no clear need for form factors. The insertion of form factors will probably change the values of the off-shell parameters, and thus it is fair to assume that the off-shell parameters and the ω exchange may be mocking up for us effects of form factors.

In Figs. 6–11, we show the results of our fit with $g_{1\Delta}=4.56$, $g_{2\Delta}=5.49$, $Z=-0.24$, $Y=-0.53$, and $X=2.39$ using Olsson's unitarization method. The data are from BD (circles) and PS (triangles). The long-dashed line is the PV nucleon Born contribution, the short-dashed line (when shown) is the PV$+\omega$ result and the solid line is the total result. If the short-dashed line is not shown, the ω contribution is small. We find sizable ω contributions for the $M_{1-}^{1/2}$, $M_{1+}^{1/2}$, and $M_{1-}^{3/2}$ multipoles

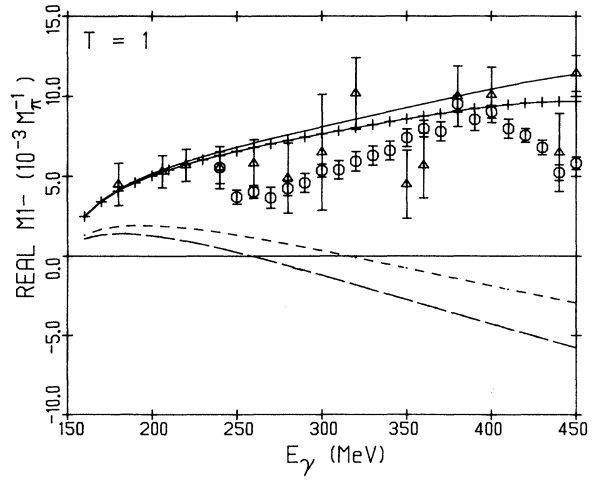

FIG. 8. Real part of $M_{1-}^{1/2}$. Data as in Fig. 2. The long-dashed line is the PV Born, short-dashed is the PV nucleon Born $+\omega$, solid line is the PV nucleon Born $+\omega+\Delta$, and the solid line with a plus through it is the PV nucleon Born $+\omega+\Delta+P_{11}(1440)$.

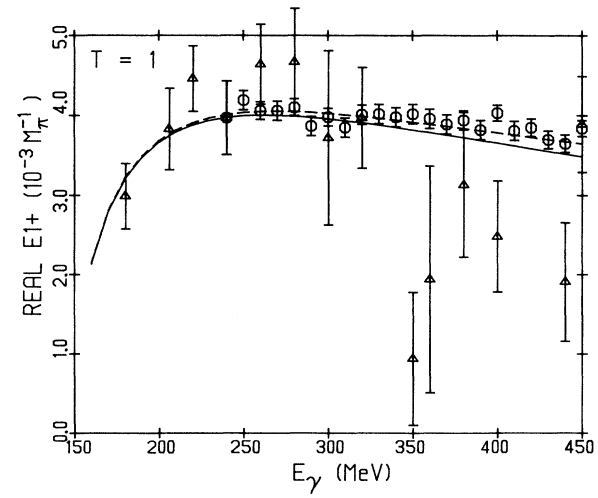

FIG. 10. Real part of $E_{1+}^{1/2}$. Curves and data same as Fig. 6.

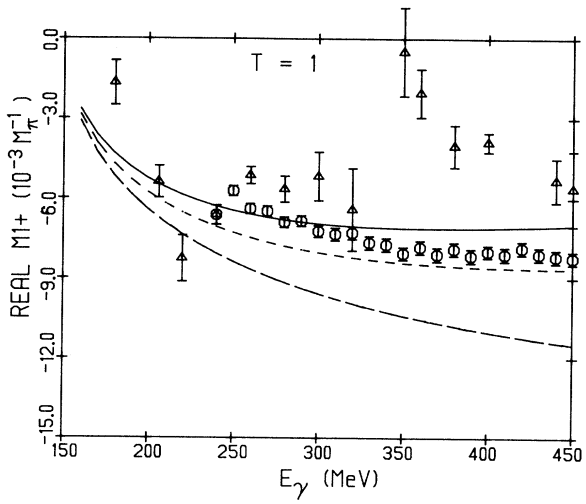

FIG. 11. Real part of $M_{1+}^{1/2}$. Curves and data same as Fig. 9.

under the assumption $g_{\omega 1} = -g_{\omega 2} = 7.98$. Most of these multipoles receive sizable nonresonant Δ contributions. In Fig. 8 we show the large u-channel Δ contribution to the $M_{1-}^{1/2}$ multipole. The Δ contribution to this multipole is largely independent of the off-shell parameters, and therefore is primarily due to the spin-$\frac{3}{2}$ part of the field.

We also shown in Fig. 8 the effect of the Roper $[P_{11}(1440)]$ resonance to the $M_{1-}^{1/2}$ in the zero width approximation, using the parameters of the Particle Data Group.[31] In this energy region, the Roper resonance produces about a 10% effect on this multipole. *This multipole deserves more theoretical and experimental investigation as it is the multipole that should first show deviations from Watson's theorem due to inelasticities in the P_{11} channel.*

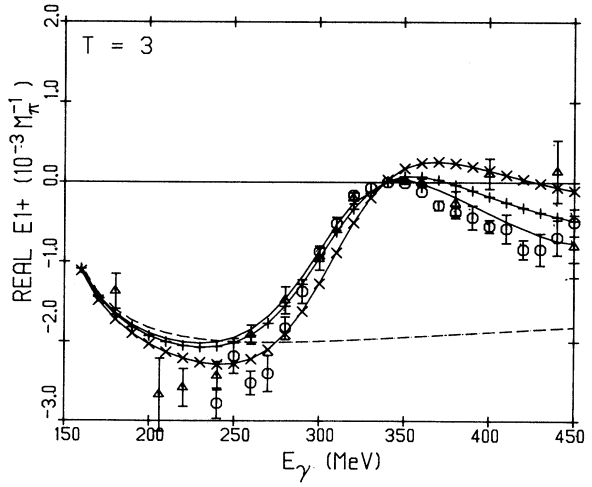

FIG. 12. Real part of $E_{1+}^{3/2}$. Data same as Fig. 2. The dashed line is the PV nucleon Born; the solid line is the total using Olsson's unitarization method; the solid line with a plus through it is the total using the K matrix, and the solid line with $\times$ through it is the total using Noelle's method.

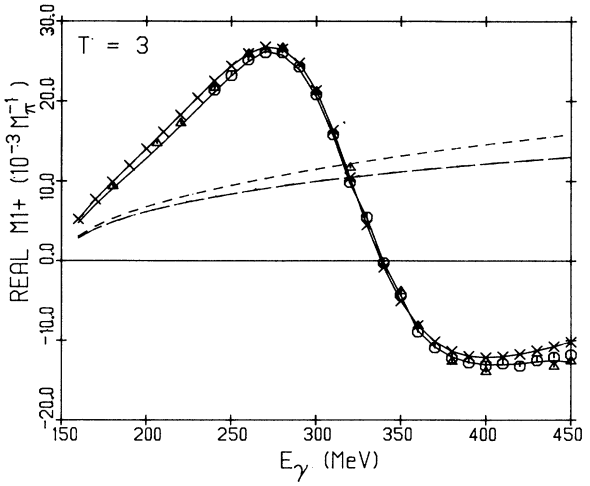

FIG. 13. Real part of $M_{1+}^{3/2}$. Data same as Fig. 2. The long dashed line is the PV Born, short dashed is the PV nucleon Born $+\omega$, the solid line is the total using Olsson's method and solid line with $\times$ through it is the total using Noelle's method. The K-matrix result falls between Olsson's and Noelle's lines and is not shown.

C. Resonant multipoles

The constraint of Watson's theorem has a small effect in the background multipoles, but it is crucial for the resonant multipoles. For all data sets except PS, we have used the phase shifts given by BD, and this may account for some of the poorness of fit to the other data sets (Ref. 29). PS have given the real and imaginary parts of the multipoles, and in fitting their data we use their phase shifts. Grushin *et al.* have not used Watson's theorem in their analysis, thereby obtaining an independent estimate of the imaginary part of the amplitude. The errors for the imaginary part are quite large, and thus it is difficult to say to what degree Watson's theorem is to be corrected. Since we assume Watson's theorem to be valid, and since the errors obtained by GRU are large, we simply use the phase shifts of BD in conjunction with the former's real part of the multipoles. Recall that small violations of Watson's theorem are expected even below the two-pion threshold due to the pion mass difference and Compton scattering.

1. $g_{1\Delta}$

Within a given data set and unitarization method, $g_{1\Delta}$ is determined to within about ± 0.10, or about 2%. This variation is due to uncertainties in the ω couplings; the error given by MINUIT for $g_{1\Delta}$ is typically $\approx 1 \times 10^{-2}$. If the data set MIR is excluded, then the different data sets give the same $g_{1\Delta}$ to within ± 0.1, using the same unitarization method. For example, using Olsson's unitarization procedure (OL), with $g_{\omega 1} = -g_{\omega 2} = 7.98$ and excluding the MIR data set, we get $g_{1\Delta} = 4.70 \pm 0.11$, whereas including the MIR data gives $g_{1\Delta} = 4.57 \pm 0.30$. Similar results hold for other unitarization procedures. The un-

certainty in $g_{1\Delta}$ is due mostly to the unitarization methods. The average of all data sets gives $g_{1\Delta}=5.01\pm0.22$ for the K matrix (K), and $g_{1\Delta}=5.72\pm0.27$ for Noelle's method (N), and the overall average is 5.10 ± 0.55, with a range from 4.06 to 5.93.

The dependence of $g_{1\Delta}$ on the unitarization procedure can easily be understood. The $M_{1+}^{3/2}$ is dominated by the s-channel Δ contribution and this contribution comes primarily from $g_{1\Delta}$. Thus ignoring the background the $g_{2\Delta}$ contributions, we would have

$$M_{1+}^{3/2} \propto \frac{g_{1\Delta} g_{\pi N\Delta}}{s - M_\Delta^2 + iM_\Delta \Gamma_\Delta} . \tag{58}$$

At resonance, using $\Gamma_\Delta \propto g_{\pi N\Delta}^2$, we would obtain

$$M_{1+}^{3/2} \propto \frac{g_{1\Delta}}{g_{\pi N\Delta}} . \tag{59}$$

Therefore, as $g_{\pi N\Delta}$ becomes large, so should $g_{1\Delta}$ for a given value of the multipoles. We shall discuss below why this does not work too well for $g_{2\Delta}$. Recalling that $g_{\pi N\Delta}=1.935$, 2.1643, and 2.4604 for OL, K, and N, respectively, we obtain from BD's data $g_{1\Delta}/g_{\pi N\Delta}=2.36$, 2.31, and 2.32 for the OL, K, and N unitarization methods, respectively. Similar results hold for other data sets, but the value of $g_{1\Delta}/g_{\pi N\Delta}$ is different than for BD's data. We emphasize that the value of $g_{1\Delta}/g_{\pi N\Delta}$ is well fixed, despite large uncertainties in the ω couplings and the off-shell parameters.

2. $g_{2\Delta}$

The ratio $g_{2\Delta}/g_{\pi N\Delta}$ is not nearly as constant as $g_{1\Delta}/g_{\pi N\Delta}$, and for BD's data the trend is the opposite; $g_{2\Delta}$ decreases as $g_{\pi N\Delta}$ increases. This is indicating that the background multipoles, which receive a contribution proportional to $g_{2\Delta}g_{\pi N\Delta}$, are playing a large role in the determination of $g_{2\Delta}$. Indeed if we choose some values of the off-shell parameters and fit $g_{1\Delta}$ and $g_{2\Delta}$ to just the $M_{1+}^{3/2}$ and $E_{1+}^{3/2}$, we find that $g_{2\Delta}/g_{\pi N\Delta}$ is fairly constant for BD's data. We should point out that the procedure of fitting $g_{1\Delta}$ and $g_{2\Delta}$ to just the resonant multipoles of BD gives vastly different values of $g_{2\Delta}$ compared to fitting all multipoles. The other data sets do *not* exhibit a large difference for the value of $g_{2\Delta}$ when fitting all the multipoles or just the resonant multipoles.

Our final results are $g_{2\Delta}=5.24\pm0.61$, 5.71 ± 0.43, and 5.47 ± 1.27 for the OL, K, and N unitarization methods, respectively, with a global average of 5.41 ± 0.85 and a range of 3.34 to 6.54.

3. *Truncated fits*

Truncating the fits to $W\approx1230$ MeV has little effect on $g_{1\Delta}$ giving a global average of $g_{1\Delta}=5.00\pm0.54$ with a range of 3.97 to 5.83. $g_{2\Delta}$ is slightly increased to $g_{2\Delta}=6.33\pm0.56$ with a range from 5.34 to 7.09. The truncation effects are largest for BD's data.

D. Transition amplitudes

The $M1$ amplitude, and consequently $A_{1/2}$ and $A_{3/2}$, is determined primarily by $g_{1\Delta}$. As can be seen from Eq. (3), the $g_{2\Delta}$ contribution is about 5% of the $g_{1\Delta}$ contribution. Our global averages are

$$M1-289\pm37, \quad A_{1/2}=-136\pm16 ,$$

$$A_{3/2}=-256\pm34 ,$$

all in the standard units of 10^{-3} GeV$^{-1/2}$. Within a given unitarization method, the "errors" on these quantities are about ±5 if the MIR data are not included, and about ±15 if the MIR data are included.

The $E2$ transition moment, and therefore the EMR, is not well determined. Our global averages are

$$E2=-5.71\pm2.73 ,$$

$$E2/M1=-(2.00\pm0.67)\% ,$$

where $E2$ is in units of 10^{-3} GeV$^{-1/2}$. The energy at which $R_{\rm EM}$ goes to zero is $\tilde{W}\gtrsim1500$ MeV, implying that $R_{\rm EM}<0$ for $W<\tilde{W}$.

There seems to be *no* correlation between χ^2_{ME} and $g_{1\Delta}$, $g_{2\Delta}$. If we arbitrarily average those values of $g_{1\Delta}$ and $g_{2\Delta}$ which correspond to a $\chi^2_{ME}\lesssim100$, then we obtain $g_{1\Delta}=5.14\pm0.46$ and $g_{2\Delta}=5.37\pm0.98$, in excellent agreement with the averages in Table I(a).

The results of $M1$, $A_{1/2}$, and $A_{3/2}$ from the truncated fits are in agreement with the full fits:

$$M1=280\pm37, \quad A_{1/2}=-135\pm17 ,$$

$$A_{3/2}=-238\pm31 .$$

The results for $E2$ and the EMR are slightly reduced in magnitude, and slightly better determined;

$$E2=-3.21\pm1.44 ,$$

$$E2/M2=-(1.12\pm0.44)\% .$$

E. Observables

In Figs. 14–23 we compare our results with the differential cross section ($d\sigma/d\Omega$), photon asymmetry (Σ), recoil nucleon polarization (P), and target asymmetry (T) at various energies and angles for the reactions $\gamma p\to p\pi^0$ and $\gamma p\to n\pi^+$. The agreement with the data is generally very good, although there are a few discrepancies. The data are from the Bonn compilation of photoproduction data,[52] Get'man *et al.*,[53] and Belyeav *et al.*[54] In these figures we show comparisons of predictions of $d\sigma/d\Omega$, Σ, P,and T for different unitarization methods and different multipole data sets. The solid line in these figures is obtained from the fit of BD's data using Olsson's unitarization method, and generally is in the best agreement with the data. The short-dashed line is obtained from Noelle's method, again fitted to BD's data. We see that Noelle's method leads to larger cross sections than Olsson's method, which is a reflection of the fact that the $M_{1+}^{3/2}$ (see Fig. 13) is larger in Noelle's method than in Olsson's method. The dash-dotted curve arises

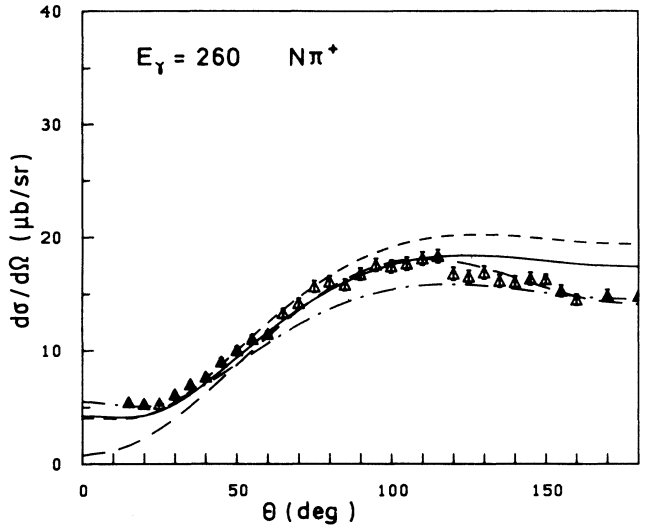

FIG. 14. Differential cross section in microbarns per steradian for $N\pi^+$ vs cm angle (in degrees) at a photon laboratory energy, E_γ, of 260 MeV. The data are from the Bonn compilation (Ref. 52). The solid curve is calculated using Olsson's unitarization method with the parameters fitted to BD's data [Table I(a), row 1], the short-dashed curve is calculated using Noelle's method with the parameters fitted to BD [Table I(a), row 3], and the dashed-dotted curve is calculated using Olsson's method with the parameters fitted to MIR [Table I(a), row 10]. The long-dashed curve includes only the S and P wave contributions to the solid curve.

from using Olsson's unitarization method, but fitted to the data of MIR. Again, the reason that this cross section is smaller than the other two is a reflection that the $M_{1+}^{3/2}$ is smaller in MIR's data than in BD's data (see Table V). We also show for π^+ production (Figs. 14–16 and 19–21) the predictions when only S and P waves (long-dashed line) are kept in the calculation of the ob-

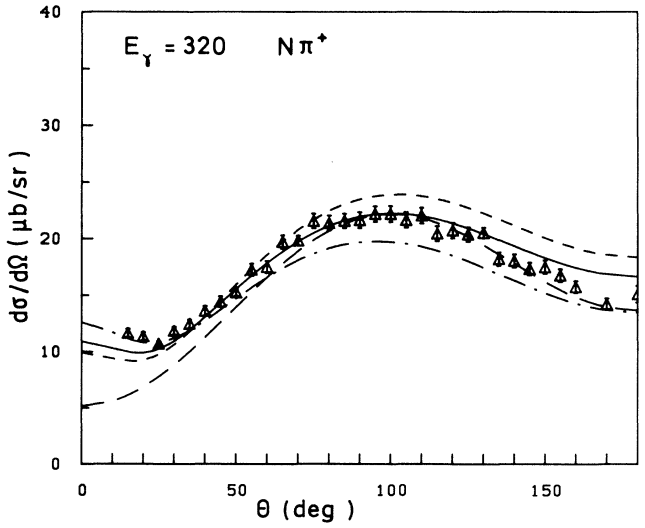

FIG. 15. Same as Fig. 14 with $E_\gamma = 320$ MeV.

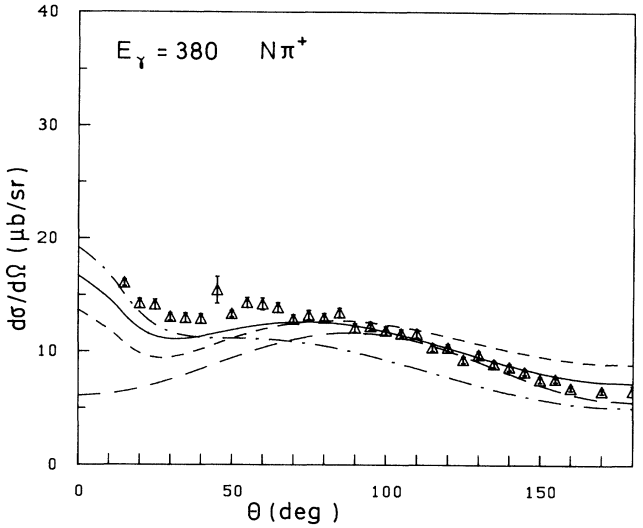

FIG. 16. Same as Fig. 14 with $E_\gamma = 380$ MeV.

servables using Olsson's method with the parameters fitted to BD's data. For π^0 production, the higher partial waves are a small effect, and then only at forward and backward angles.

We remark here that *all* partial waves resulting from the PV nucleon Born terms and vector-meson exchanges have been included in the calculations of the observables. This is achieved by subtracting off the nonunitarized multipoles (i.e., the tree approximation to the multipoles) from the $\mathcal{F}$'s,[16] and adding on the unitarized multipoles. This can also be done for the Δ contribution, but should be a small effect. This is supported by the fact that the higher partial waves for π^0 production resulting from the u-channel nucleon exchange are small. In fact, the

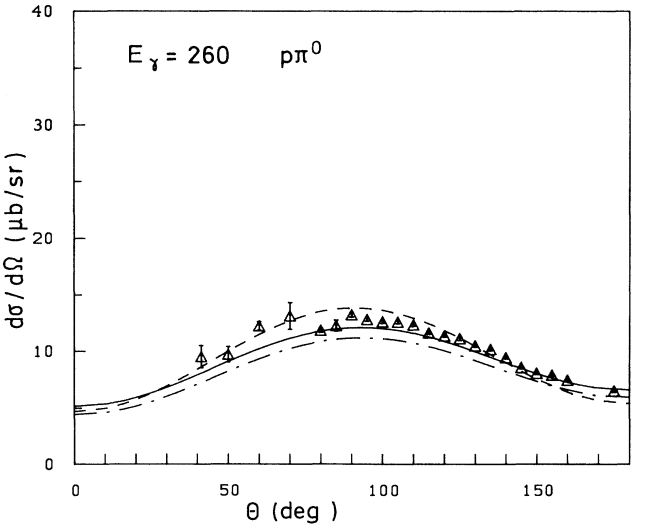

FIG. 17. Differential cross section for $p\pi^0$ at $E_\gamma = 260$ MeV. Data and curves as in Fig. 14, except the contribution from only the S and P waves is not shown since it is nearly the same as the full calculation.

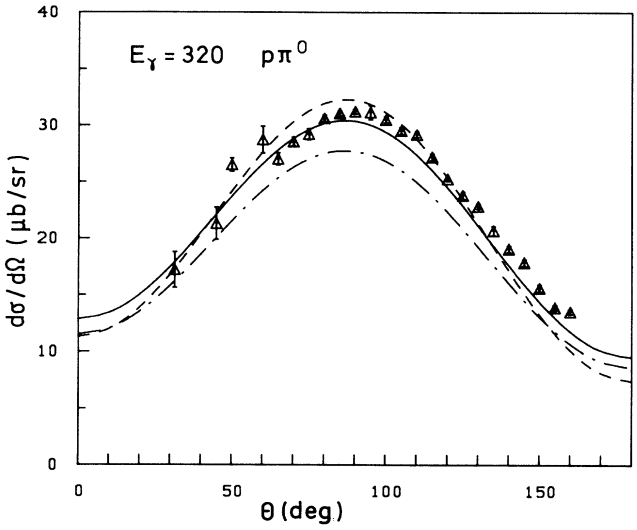

FIG. 18. Same as Fig. 17 except $E_\gamma = 320$ MeV.

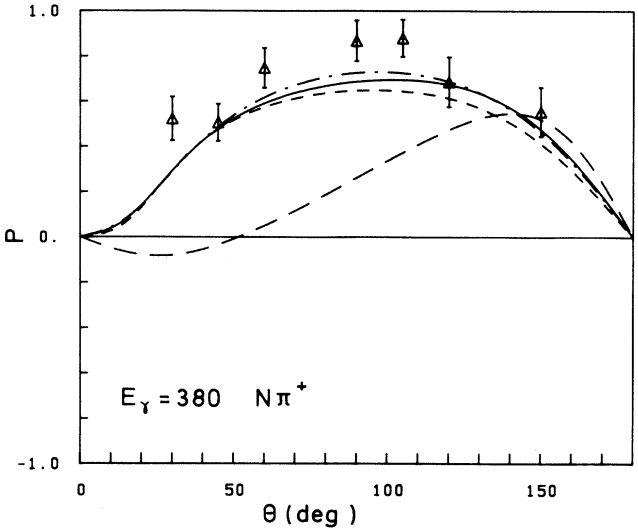

FIG. 20. Recoil nucleon polarization for $N\pi^+$ vs cm angle at $E_\gamma = 380$ MeV. Curve and data as in Fig. 19.

higher partial waves for pion photoproduction are dominated by the t-channel pion exchange [in the gauge $\epsilon_\mu = (0, \epsilon)$]. It is interesting to note that T (Fig. 21) is not very sensitive to the higher partial waves. Although we may convince ourselves that this is correct by examining the manner in which the $\mathcal{F}$'s enter into the expression for T, we do not currently have a deeper physical understanding of why T is not sensitive to the higher partial waves. Finally, the differences we show here for the observables are the extremes. For example, the K-matrix predictions lie between the predictions of the Noelle and Olsson methods. Also, the fits to the MIR data give the largest variation in $g_{1\Delta}$.

F. K matrix residues

It is possible[29] to extract from the multipole data sets the K-matrix pole position and residues for πN elastic scattering and pion photoproduction in a model-independent manner. For the resonant partial wave and multipoles we have, for the K-matrix elements,

$$K_{\gamma\pi} = \frac{A}{M_{33} - W} + B \ , \tag{60}$$

$$K_{\pi\pi} = \frac{C}{M_{33} - W} + D \ , \tag{61}$$

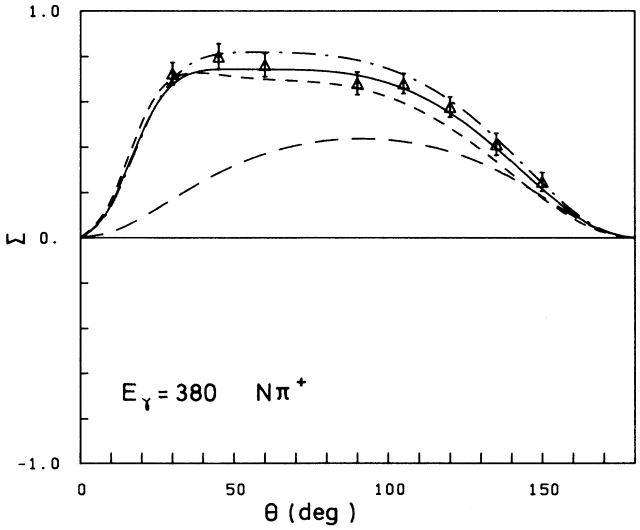

FIG. 19. Photon asymmetry for $N\pi^+$ vs cm angle at $E_\gamma = 380$ MeV. The calculation is done using the unitarization method of Olsson with the parameters fitted to BD's data. The data are from Ref. 53.

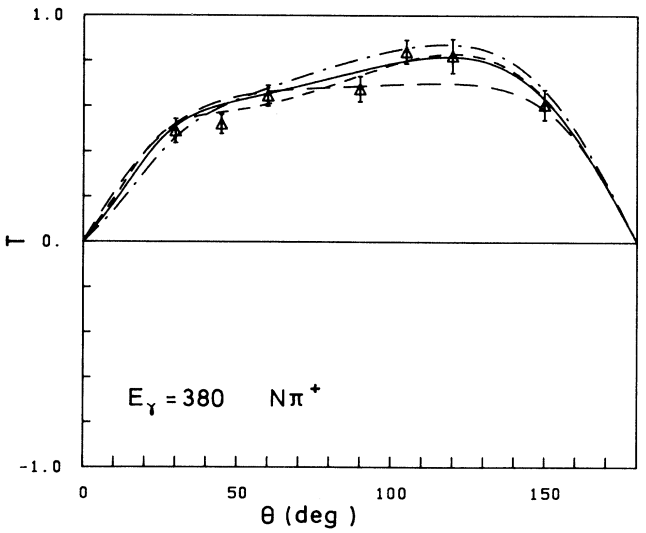

FIG. 21. Target asymmetry for $N\pi^+$ vs cm angle at $E_\gamma = 380$ MeV. Curve and data as in Fig. 19.

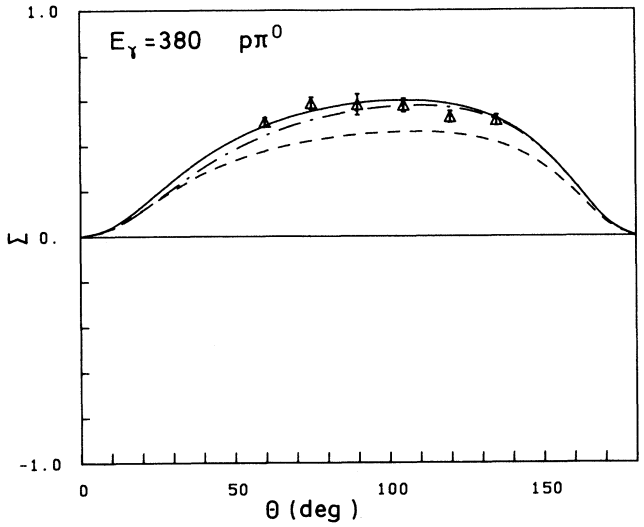

FIG. 22. Photon asymmetry for $p\pi^0$ vs cm angle at $E_\gamma=380$ MeV. Curves and data as in Fig. 17.

where we ignore Compton corrections and M_{33} is the energy at which the δ_{33} phase shift passes through 90°. Evidently, $C=-\mathrm{Re}(K_{\pi\pi})$ and $A=-\mathrm{Re}(K_{\gamma\pi})$ (this is true for both the $M_{1+}^{3/2}$ and the $E_{1+}^{3/2}$). Here we assume A,B,C,D to be smooth functions of W. Converting to the T matrix, treating the electromagnetic channel as a perturbation to the strong channel, and adding necessary kinematical factors, we find, for the resonant partial wave $f_{1+}^{3/2}$,

$$\frac{d}{dW}(\mathrm{Re}f_{1+}^{3/2})=-\frac{1}{qC} \tag{62}$$

and, for either resonant multipole $A_{\gamma\pi}$,

$$\chi=\frac{d}{dW}(\mathrm{Re}A_{\gamma\pi})=\frac{-A}{\sqrt{qk}\,C^2}\ , \tag{63}$$

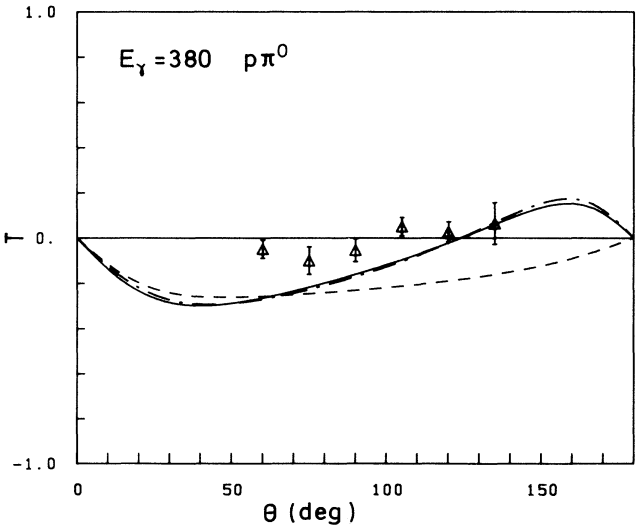

FIG. 23. Target asymmetry for $p\pi^0$ vs cm angle at $E_\gamma=380$ MeV. Curves as in Fig. 17 and data from Ref. 54.

TABLE VI. A comparison with experiment of the K-matrix residue parameters (in units of $10^{-3}m^{-1}$ MeV^{-1}) predicted by various fits.

Data	Unit	χ_E (10^{-3})	χ_M
BD Expt		4.91±2.94	−0.667±0.02
BD22	OL	12.28	−0.661
BD22	K	13.99	−0.661
BD22	N	25.60	−0.652
BD7	OL	5.48	−0.666
BD7	K	4.69	−0.665
BD7	N	9.34	−0.649
PS Expt		5.89±7.88	−0.693±0.030
PS11	OL	9.82	−0.683
PS11	K	8.88	−0.677
PS11	N	11.36	−0.652
PS5	OL	7.82	−0.678
PS5	K	5.66	−0.651
PS5	N	6.84	−0.626
GET Expt		7.68±2.60	−0.635±0.013
GET10	OL	12.44	−0.652
GET10	K	12.24	−0.661
GET10	N	15.82	−0.652
GET5	OL	11.87	−0.651
GET5	K	10.16	−0.655
GET5	N	11.48	−0.642
MIR Expt		6.83±1.44	−0.662±0.013
MIR11	OL	12.15	−0.563
MIR11	K	8.72	−0.606
MIR11	N	12.09	−0.589
MIR5	OL	12.29	−0.542
MIR5	K	6.21	−0.592
MIR5	N	7.23	−0.572
GRU Expt		12.06±5.20	−0.642±0.147
GRU6	OL	13.76	−0.629
GRU6	K	11.24	−0.679
GRU6	N	12.55	−0.666

where all quantities are evaluated at $W=M_{33}$. From the phase shifts given by BD, we find $C\approx 57.1$ MeV. In Table VI we compare the predictions of χ_M and χ_E obtained from the various fits in Tables I and II with those extracted directly from the data using a Lagrange interpolating function.[55] The notation is the same as Table I, and $\chi_{M,E}$ are in units of $10^{-3}m^{-1}$ MeV^{-1}. The errors are obtained by a combination of propagation of the *quoted* error on the multipole, and an estimate of the accuracy of the interpolating function. See Ref. 29 where the discrepancies amongst the multipole data sets are taken into account, and an additional relation for A is given.

We see that the values of χ_E obtained in various fits are often not in agreement with experiment. If we consider only the fits in which χ_E is in agreement with the data, we find a slightly smaller $E2$, but still a large spread, $E2=-3.5\pm1.8$. The spread in values is not only a reflection of the fact that χ_E is different for different data sets, but also of the fact that $E2$ is different in the different unitarization methods.

To illustrate this model dependence in the extraction of

the resonant parameters it is useful to compare the fits to BD's truncated data set using the K and OL methods of unitarization. These two methods give quite similar results for $\chi_{M,E}$, and yield good agreement with the experimental values.[29] In particular, OL gives $\chi_E=5.48\times10^{-3}$ and $\chi_M=-0.666$ while K gives $\chi_E=4.69\times10^{-3}$ and $\chi_M=-0.665$. Comparing the transition amplitudes as defined by (2) and (3) we see that the agreement is rather poor; OL gives $E2=-0.97$ and $M1=251$, while K gives $E2=-1.99$, and $M1=284$. The EMR is also quite different, OL gives -0.39% while K gives -0.70%.

To further illustrate the model dependence of the quantities $E2$ and $M1$, consider our fit to BD's data using OL with $g_{\omega1}=g_{\omega2}=0$ [Table I(b)]. In this fit we obtain $E2=+0.3$, and near the resonance the fit to the experimental $E_{1+}^{3/2}$ is very good, the theory is within the error bar of every data point in the energy range $320\le k_l\le390$. Despite the change in sign of $E2$, this fit gives $\chi_E=3.6\times10^{-3}$ which is in agreement with experiment. Thus, by changing the background we find a fit in which $E2$ changes sign, but the K-matrix residue does not change sign and is in agreement with experiment. Doing the same fit with K also gives a χ_E in agreement with experiment and an excellent fit to the $E_{1+}^{3/2}$ near resonance, but in this case we obtain $E2=-1.6$.

The fact that $E2$ and $M1$ can vary so much when χ_E and χ_M remain stable illustrates the model dependence of the decomposition of the amplitude into a resonant piece, which we hope to compare with baryon models, and a nonresonant piece. To be explicit, in the K-matrix unitarization method, the expressions for $A(M_{33})$ and $C(M_{33})$ are

$$C=\frac{g_{\pi N\Delta}^2(E_f+M)q^3}{24m^2M_{33}\pi}\ , \tag{64}$$

$$A_M=\frac{eS_1S_2(qk)^{3/2}g_{\pi N\Delta}}{96\pi M_{33}Mm(M_{33}+M)}\times\left[g_{1\Delta}(3M_{33}+M)-g_{2\Delta}\frac{M_{33}(M_{33}-M)}{2M}\right]\ , \tag{65}$$

and

$$A_E=\frac{-eS_1S_2(qk)^{3/2}g_{\pi N\Delta}(M_{33}-M)}{96\pi M_{33}Mm(M_{33}+M)}\left[g_{1\Delta}-g_{2\Delta}\frac{M_{33}}{2M}\right]\ , \tag{66}$$

where all kinematical variables are evaluated at $W=M_{33}$.

In *this model* the dependence on $\tan\delta_B$ and A_B drops out and the residues are determined by $g_{\pi N\Delta}$, M_Δ, $g_{1\Delta}$, and $g_{2\Delta}$. Furthermore, $M_\Delta=M_{33}$, in contrast to the other unitarization cases, OL ($M_\Delta<M_{33}$) and N ($M_\Delta>M_{33}$). In the procedures of Olsson and Noelle, the background does not drop out at the K-matrix pole. In Noelle's method,

$$A=\frac{N}{\cos\delta_B}\ , \tag{67}$$

and, in Olsson's method,

$$A\propto N\cos(\delta_p-\delta_B)\ . \tag{68}$$

Thus, in Olsson's and Noelle's methods the K-matrix residues are functions not only the resonance parameters, but also the parameters, such as $g_{\pi NN}$, which describe the background in that model.

G. Comparison with models

In Table VII we compare our results, obtained by averaging the full and truncated fits, with the predictions of the nonrelativistic quark model,[56] the chiral bag model,[7] the Skyrme model,[8] a relativized quark model,[5] and a hybrid model.[9] This list certainly is not exhaustive, and variations within a model will certainly produce variations in $E2$ and $M1$. For example, it has been estimated that expanding the basis in the nonrelativistic quark model will change the EMR in this model to $\approx-0.7\%$,[5] bringing it into better agreement with our results.

The physics of the $E2$ transition in these models is quite different. The $E2$ might arise solely by a photon-pion coupling,[8] a photon-quark coupling,[56,5] or a combination of both.[7,9] Furthermore, in the quark models the $E2$ may be the result of (1) d-state admixture com-

TABLE VII. A comparison of our results with various baryon models. A dash (–) means that the particular result is not known to us.

Source	$M1$	$E2$	EMR (%)	$A_{1/2}$	$A_{3/2}$
Nonrelativistic quark model, Refs. 4 and 53	206	−1.96	−0.4	−100	−180
Chiral bag model, Ref. 6	290	−2.82	−0.9	−141	−254
Skyrme model, Ref. 7	284	−8.80	−2.90	−129	−254
Relativized quark model, Ref. 4	–	–	−0.2	–	–
Hybrid model, Ref. 8	229	−10.10	−4.4	−99.4	−207
This work	285±37	−4.60±2.58	−1.57±0.72	−135±16	−251±33

ponents in the nucleon and Δ arising from one-gluon and/or one-pion exchange, (2) relativistic effects (nucleon and Δ assumed "spherical" in their respective rest frames), or (3) the pion cloud. Given the differences amongst these models, it is satisfying to see that they all give the same sign and order of magnitude for the EMR. This is an important conclusion of our work: *the EMR extracted in our work agrees in sign and order of magnitude with most realistic models of the nucleon and* Δ. However, the uncertainties in the hadron model estimates for the transition amplitudes are currently greater than the results extracted in this work. Improvements in the former are needed to motivate better quality experiments possible in the emerging facilities.

V. CONCLUSIONS

We have investigated pion photoproduction in the Δ (1232) resonance region using an effective Lagrangian with a number of unitarization methods. Our model contains five parameters describing the Δ interactions which have been fitted to the various multipole data sets. Our model is in good agreement with the multipoles and with the observables, for all channels, and thus our derived amplitude that describes pion photoproduction well off nucleons can be used as input to a nuclear pion-photoproduction calculation.

We have found that within a given unitarization method we have adopted, the $M1$ transition amplitude for the $\gamma \rightarrow N\Delta$ process is determined to within about 5%. The χ^2 for the $M_{1+}^{3/2}$ multipole fits that we have achieved are, in some cases, quite large, but there are large discrepancies amongst the multipole data sets which need to be resolved. The $E2$ transition amplitude is determined to within about 25% in a given unitarization method that we have used, reflecting the relatively large errors for the $E_{1+}^{3/2}$ multipole.

Our determination of the resonant amplitudes for the $\gamma \rightarrow N\Delta$ transition can be summarized as follows:

$$M1 = 285 \pm 37, \quad E2 = -4.60 \pm 2.58 ,$$

$$E2/M1 = -(1.57 \pm 0.72)\% ,$$

$$A_{1/2} = -135 \pm 16, \quad A_{3/2} = -251 \pm 33 ,$$

where the amplitudes are in the usual units of 10^{-3} $\mathrm{GeV}^{-1/2}$. These averages and errors are taken from both the full and truncated fits including all data sets and unitarization methods. Thus, the above errors reflect the uncertainties in the experimental multipole base, and theoretical uncertainties arising from the ambiguities of the unitarization method.

The extracted amplitudes given above are of the same order of magnitude as predicted by realistic hadron models, even as the latter contain theoretical uncertainties that are considerably large, exceeding those of our analysis. It is still interesting to see that our extracted $E2$ amplitude is *nonzero,* as predicted by realistic hadron models, in disagreement with the null value in the naive SU(6), $\mathrm{SU}_W(6)$ cases; its negative sign relative to the $M1$ amplitude is also in accord with realistic theoretical works. The significance of this sign varies from one specific model to another, and we are unable to sort them out. It is important to stress here that the ratio of the $E2$-to-$M1$ amplitudes for the real photon is very different from that expected in the perturbative QCD regime, thereby suggesting important dynamical effects as we go away from the real-photon point.

In the future we can only hope that a more reliable multipole data base can be obtained by more refined experiments and analyses in new cw machines. However, even when this becomes available, one will still be dealing with the model-dependent extraction of the resonant parameters. In this work we have shown that different unitarization procedures give $M1$ amplitudes that differ by about $\pm 20\%$ and $E2$ amplitudes that differ by $\pm 60\%$. Possibly the χ^2 could be used as a basis to rule out a given unitarization method, but we find that different methods work best for different data sets currently available. Since we cannot judge which set is best, we have treated all sets on equal footing and have given equal weight to all unitarization procedures. It is perhaps worth noting that Noelle's method never gives the best fit (as compared to the other methods) to any data set.

The model dependence involved in the extraction of resonance parameters is an old problem. The ultimate test of hadron models will be a direct comparison with the strong and electromagnetic scattering data.[57]

Apart from the precise relation between the resonant parameters extracted here and those calculated in topical baryon models, there are several open questions. Since we can definitely rule out the gauge coupling $g_{2\Delta}=0$, in this approach, we conclude that the constraints derived by Nath and Bhattacharyya[19] on the parameters $g_{2\Delta}$, Y, and Z are too restrictive to apply to transitions between composite particles. Unfortunately we do not know how to predict the parameters X, Y, and Z starting from a composite model of hadrons. Further work needs to be done on the role of the σ term in pion photoproduction in the Δ region. The σ term seems to be important for threshold π^0 production. Finally, calculation of the one-loop corrections using chiral perturbation theory would be an interesting theoretical step.

ACKNOWLEDGMENTS

We thank M. Benmerrouche for many discussions and Professor A. Donnachie for communication. We are grateful to the Rensselaer Polytechnic Institute Intermediate Energy Group for computational support. This research was supported in part by the U.S. Department of Energy under Contract Nos. DE-AC02-83-ER40114.A002 and DE-AC02-83-ER40114.A003, and under Grant No. DE-FG02-88ER40448.A002, to N.C.M. Part of this work constitutes part of the Ph.D. thesis of R.M.D. at Rensselaer.

APPENDIX

For completeness we give the amplitudes for the PV Born terms, ω and ρ exchange, and Δ exchange. The invariant amplitudes $A_i(s,t,u)$ are as defined in Ref. 16, except we use the conventions of Bjorken and Drell.[58]

The contribution from the PV Born terms may be written as

$$\mathbf{A}^{+,0,-}=\left[\frac{1}{s-M^2}+\bar{\xi}\frac{1}{u-M^2}\right]\Gamma+\Gamma^{\mathrm{PV}}\ , \tag{A1}$$

where $\mathbf{A}\equiv(A_1,A_2,A_3,A_4)$, $\Gamma\equiv(\Gamma_1,\Gamma_2,\Gamma_3,\Gamma_4)$, $\bar{\xi}=\xi^{+,0,-}\mathrm{diag}(1,1,-1,1)$, $\xi^{+,0,-}=(1,1,-1)$,

$$\Gamma_1^{\pm,0}=\frac{efM}{m}\ , \tag{A2}$$

$$\Gamma_2^{\pm,0}=\frac{2efM}{m(m^2-t)}\ , \tag{A3}$$

$$\Gamma_3^{\pm,0}=\Gamma_4^{\pm,0}=-\frac{ef\kappa^{+,0}}{m}\ , \tag{A4}$$

$$\Gamma_1^{\mathrm{PV}}=\tfrac{1}{2}(1+\xi^{+,0-})\frac{ef\kappa^{+,0}}{mM}\ , \tag{A5}$$

and

$$\Gamma_{2,3,4}^{\mathrm{PV}}=0\ . \tag{A6}$$

Also, $\kappa^+=(\kappa_p-\kappa_n)/2$ and $\kappa^0=(\kappa_p+\kappa_n)/2$. s, t, and u are the usual Mandelstam variables, and the other quantities are as previously defined in the text.

The contributions from the vector mesons are

$$A_1^{+(0)}=-\frac{e}{m}\frac{\lambda_{\omega(\rho)}g_{\omega(\rho)2}}{2M}\frac{t}{M_{\omega(\rho)}^2-t}\ , \tag{A7}$$

$$A_2^{+(0)}=\frac{e}{m}\frac{\lambda_{\omega(\rho)}g_{\omega(\rho)2}}{2M}\frac{1}{M_{\omega(\rho)}^2-t}\ , \tag{A8}$$

$$A_3^{+(0)}=0\ , \tag{A9}$$

and

$$A_4^{+(0)}=\frac{e}{m}\lambda_{\omega(\rho)}g_{\omega(\rho)1}\frac{1}{M_{\omega(\rho)}^2-t}\ . \tag{A10}$$

The $g_{1\Delta}$ contribution is

$$\mathbf{A}^{+,0,-}=\left[\frac{1}{s-M_\Delta^2}+\bar{\xi}\frac{1}{u-M_\Delta^2}\right]\Delta(t)+\mathbf{A}_{np}^{+,0,-}\ , \tag{A11}$$

with

$$\Delta_1=\frac{\delta^{+,0,-}}{8}\left[4t+\frac{4M}{3M_\Delta}(M_\Delta^2-M^2+2m^2)+\frac{4M^2}{3M_\Delta^2}(M_\Delta^2-M^2+m^2)\right]\ , \tag{A12}$$

$$\Delta_2(t)=-\delta^{+,0,-}\ , \tag{A13}$$

$$\Delta_3(t)=\frac{\delta^{+,0,-}}{8}\left[-(2M+4M_\Delta)+\frac{4M^2}{3M_\Delta}+\frac{2M}{3M_\Delta^2}(M_\Delta^2-2M^2+2m^2)\right]\ , \tag{A14}$$

$$\Delta_4(t)=\frac{\delta^{+,0,-}}{8}\left[6M+4M_\Delta+\frac{4M^2}{3M_\Delta}+\frac{2M}{3M_\Delta^2}(M_\Delta^2-2M^2+2m^2)\right]\ , \tag{A15}$$

and

$$\delta^{+,0,-}=\frac{(-2,0,1)eg_{\pi N\Delta}g_{1\Delta}}{6mM}\ . \tag{A16}$$

The only nonzero components of $\mathbf{A}_{np}^{+,0,-}$ are

$$A_{1,\mathrm{NP}}^{+}=-\frac{\delta^+}{3M_\Delta^2}\left[\frac{\beta}{4}(\alpha-1)(t-m^2)+\beta m^2-M(M+M_\Delta)\right]\ , \tag{A17}$$

$$A_{4,\mathrm{NP}}^{+}=-\frac{\delta^+}{3M_\Delta^2}\left[\alpha\beta M_\Delta+\frac{M}{2}(\alpha\beta+\alpha+\beta)\right]\ , \tag{A18}$$

$$A_{1,\mathrm{NP}}^{-}=\frac{\delta^-}{3M_\Delta^2}\left[\frac{\beta}{4}(\alpha-1)(s-u)\right]\ , \tag{A19}$$

and

$$A_{3,\mathrm{NP}}^{-}=-\frac{\delta^-}{3M_\Delta^2}\left[\alpha\beta M_\Delta+\frac{M}{2}(\alpha\beta+\alpha+\beta)\right]\ , \tag{A20}$$

where $\alpha=1+4Z$ and $\beta=1+4Y$.

The $g_{2\Delta}$ contribution can be written in the form

$$\mathbf{A}^{\pm}=\mathbf{A}_{\mathrm{P}}^{\pm}+\mathbf{A}_{\mathrm{NP}}^{\pm}\ , \tag{A21}$$

where $A_i^0=0$ for all i. We find, for the pole (P) terms,

$$A_{1,\mathrm{P}}^{+}=\frac{C^\pm}{6(s-M_\Delta^2)}\left[M(3t-2m^2)+(s-M^2)M_\Delta-\frac{s-M^2+m^2}{2M_\Delta}(s+M^2)\right]\pm s\leftrightarrow u\ , \tag{A22}$$

$$A_{2,\mathrm{P}}^{\pm}=C^\pm\frac{M_\Delta-M}{2}\left[\frac{1}{s-M_\Delta^2}\pm\frac{1}{u-M_\Delta^2}\right]\ , \tag{A23}$$

$$A_{3,\mathrm{P}}^{\pm}=\frac{C^\pm}{12(s-M_\Delta^2)}\left[(3t-2m^2)+5(s-M^2)-\frac{M}{M_\Delta}(s-M^2+m^2)\right]\mp s\leftrightarrow u\ , \tag{A24}$$

$$A_{4,\mathrm{P}}^{\pm}=\frac{C^\pm}{12(s-M_\Delta^2)}\left[(3t-2m^2)-(s-M^2)-\frac{M}{M_\Delta}(s-M^2+m^2)\right]\pm s\leftrightarrow u\ , \tag{A25}$$

where

$$C^\pm=\frac{eg_{\pi N\Delta}g_{2\Delta}\delta^\pm}{4M^2m}\ , \tag{A26}$$

$\delta^+=-\frac{2}{3}$, and $\delta^-=\frac{1}{3}$.

The nonpole (NP) terms are

$$A^{\pm}_{2,\mathrm{NP}}=0\ , \tag{A27}$$

$$A^{+}_{1,\mathrm{NP}}=\frac{C^{+}}{6M_{\Delta}^{2}}(m^{2}-t)[M(-\tfrac{1}{2}-X+Z+2ZX) -M_{\Delta}(Z+X+4ZX)] -\frac{C^{+}}{6M_{\Delta}^{2}}2Mm^{2}(1+2X)\ , \tag{A28}$$

$$A^{+}_{3,\mathrm{NP}}=\frac{C^{+}}{6M_{\Delta}^{2}}(s-u)Z(1+2X)\ , \tag{A29}$$

$$A^{+}_{4,\mathrm{NP}}=\frac{C^{+}}{6M_{\Delta}^{2}}[(m^{2}-t)Z(1+2X)-m^{2}(1+2X)]\ , \tag{A30}$$

$$A^{-}_{1,\mathrm{NP}}=\frac{C^{-}}{6M_{\Delta}^{2}}(s-u)[M(-\tfrac{1}{2}-X+Z+2XZ) -M_{\Delta}(Z+X+4XZ)]\ , \tag{A31}$$

$$A^{-}_{3,\mathrm{NP}}=\frac{C^{-}}{6M_{\Delta}^{2}}[(m^{2}-t)Z(1+2X)-m^{2}(1+2X)]\ , \tag{A32}$$

and

$$A^{-}_{4,\mathrm{NP}}=\frac{C^{-}}{6M_{\Delta}^{2}}(s-u)Z(1+2X)\ . \tag{A33}$$

Finally, the $\frac{3}{2}\rightarrow\frac{1}{2}$ spin transition can be represented by three 2×4 matrices S_x, S_y, and S_z. In our conventions, the nonzero values of these matrices are

$$S_x^{24}=-S_x^{11}=\frac{1}{\sqrt{2}}\ , \tag{A34}$$

$$S_x^{13}=-S_x^{22}=\frac{1}{\sqrt{6}}\ , \tag{A35}$$

$$S_y^{11}=S_y^{24}=-\frac{i}{\sqrt{2}}\ , \tag{A36}$$

$$S_y^{13}=S_y^{22}=-\frac{i}{\sqrt{6}}\ , \tag{A37}$$

and

$$S_z^{12}=S_z^{23}=\sqrt{2/3}\ . \tag{A38}$$

---

*Current address: Institut für Theoretische Physik III, Universität Erlangen-Nürnberg, D8520 Erlangen, West Germany.

†Current address: University of Indiana, Nuclear Theory Center, Bloomington, Indiana 47405.

[1]For recent reviews of different theoretical aspects of this topic, see papers by F. E. Close, S. Capstick, R. H. Dalitz, and N. Isgur, in *Excited Baryons 1988,* Topical Workshop on Excited Baryons, Troy, New York, 1988, edited by G. Adams, N. C. Mukhopadhyay, and P. Stoler (World Scientific, Teaneck, NJ, 1989). The article therein by N. C. Mukhopadhyay reviews the current experimental and theoretical situation for the nucleon-to-Δ electromagnetic transition.

[2]For a general survey, see, for example, *Electromagnetic Interactions of Hadrons,* edited by A. Donnachie and G. Shaw (Plenum, New York, 1978), Vols. 1 and 2. For a latest compilation of many available earlier analyses, see Particle Data Group, G. P. Yost *et al.*, Phys. Lett. B **204**, 377 (1988).

[3]R. Wittman, R. Davidson, and N. C. Mukhopadhyay, Phys. Lett. **142B**, 336 (1984).

[4]R. Davidson, N. C. Mukhopadhyay, and R. Wittman, Phys. Rev. Lett. **56**, 804 (1986).

[5]S. L. Glashow, Physica **A96**, 27 (1979); N. Isgur, G. Karl, and R. Koniuk, Phys. Rev. D **25**, 2394 (1982); S. S. Gershtein and G. V. Dzhikiya, Yad. Fiz. **34**, 1566 (1981) [Sov. J. Nucl. Phys. **34**, 870 (1981)]; M. Bourdeau and N. C. Mukhopadhyay, Phys. Rev. Lett. **58**, 976 (1987); **63**, 335 (1989); S. Capstick and G. Karl, Phys. Rev. D **41**, 2767 (1990). This last reference explores a relativized quark model. See also J. Bienkowska, Z. Dziembowski, and H. J. Weber, Phys. Rev. Lett. **59**, 624 (1987); M. Warns, H. Schröder, W. P. Pfeil, and H. Rollnik, Z. Phys. C **45**, 613 (1990).

[6]C. Carlson, Phys. Rev. D **34**, 2704 (1986).

[7]G. Kälbermann and J. M. Eisenberg, Phys. Rev. D **28**, 71 (1983).

[8]G. S. Adkins, C. R. Nappi, and E. Witten, Nucl. Phys. **B228**, 552 (1983); G. S. Adkins and C. R. Nappi, *ibid.* **B249**, 507 (1985); A. Wirzba and W. Weise, Phys. Lett. B **188**, 6 (1987).

[9]T. D. Cohen and W. Broniowski, Phys. Rev. D **34**, 3472 (1986).

[10]R. Wittman and N. C. Mukhopadhyay, Phys. Rev. Lett. **57**, 1113 (1986); R. Wittman, Ph.D. thesis, Rensselaer Polytechnic Institute, 1986.

[11]S. Weinberg, Phys. Rev. **166**, 1568 (1968).

[12]R. D. Peccei, Phys. Rev. **181**, 1902 (1969).

[13]M. G. Olsson and E. T. Osypowski, Nucl. Phys. **B87**, 399 (1975); Phys. Rev. D **17**, 174 (1978).

[14]N. Dombay and B. J. Read, Nucl. Phys. **B60**, 65 (1973).

[15]W. Rarita and J. Schwinger, Phys. Rev. **60**, 61 (1941); P. A. Moldhauer and K. M. Case, Phys. Rev. D **3**, 2153 (1971).

[16]G. F. Chew, M. L. Goldberger, F. E. Low, and Y. Nambu, Phys. Rev. **106**, 1345 (1957).

[17]The argument against double counting is given in the second article in Ref. 13. To summarize, there is some concern that higher-energy baryon exchanges might be misinterpreted as vector-meson exchanges and vice versa. Olsson and Osypowski argue that the higher baryon resonances have a small effect in the Δ region and a structure quite different from that of the vector mesons. This, in addition to the fact that the vector-meson couplings are in general agreement with the quark-model predictions, lead them to conclude that they have properly interpreted the vector-meson exchanges in this energy range.

[18]M. G. Olsson, Nucl. Phys. **B78**, 55 (1974).

[19]L. M. Nath and B. K. Bhattacharyya, Z. Phys. C **5**, 9 (1980).

[20]R. M. Davidson and N. C. Mukhopadhyay, Phys. Rev. Lett. **60**, 748 (1988).

[21]E. Mazzucato *et al.*, Phys. Rev. Lett. **57**, 3144 (1986); **60**, 749 (1988); R. Beck, Ph.D. thesis, Mainz, 1989.

[22]F. A. Berends and A. Donnachie, Nucl. Phys. **B58**, 378 (1973).

[23]W. Pfeil and D. Schwela, Nucl. Phys. **B45**, 379 (1971).

[24]V. A. Get'man, V. M. Sanin, Yu Telegin, and S. V. Shalaski, Yad. Fiz. **38**, 385 (1983) [Sov. J. Nucl. Phys. **38**, 230 (1983)].

[25]V. F. Grushin, A. A. Shikanyan, E. M. Leikin, and A. Ya Rotvain, Yad. Fiz. **38**, 1448 (1983) [Sov. J. Nucl. Phys. **38**, 881

(1983)].
[26]I. I. Miroshnichenko, V. I. Nikiforov, V. M. Sanin, P. V. Sorokin, and S. V. Shalatskii, Yad. Fiz. **32**, 659 (1980) [Sov. J. Nucl. Phys. **32**, 339 (1980)].
[27]I. Blomqvist and J. M. Laget, Nucl. Phys. **A280**, 405 (1977).
[28]P. Stoler, in *Excited Baryons 1988* (Ref. 1), p. 332.
[29]R. M. Davidson and N. C. Mukhopadhyay, Phys. Rev. D **42**, 20 (1990).
[30]H. F. Jones and M. D. Scadron, Ann. Phys. (N.Y.) **81**, 1 (1973).
[31]Particle Data Group, M. Aguilar-Benitez *et al.*, Phys. Lett. **170B**, 1 (1986).
[32]S. Kumano, Phys. Lett. B **214**, 132 (1988).
[33]A. Donnachie, in *High Energy Physics,* edited by E. H. S. Burhop (Aacdemic, New York, 1972), pp. 1–185.
[34]M. Benmerrouche, R. M. Davidson, and N. C. Mukhopadhyay, Phys. Rev. C **39**, 2339 (1989).
[35]L. M. Nath and S. K. Singh, Phys. Rev. C **39**, 1207 (1989).
[36]N. M. Kroll and M. A. Ruderman, Phys. Rev. **93**, 233 (1954).
[37]O. Dumbrajs, R. Koch, P. Pilkuhn, G. C. Oades, H. Behrens, J. J. de Swart, and P. Kroll, Nucl. Phys. **B216**, 277 (1983).
[38]For a recent discussion, see C.-Y. Ren and M. K. Banerjee, Phys. Rev. C **41**, 2370 (1990).
[39]L. M. Nath, B. Etemadi, and J. D. Kimel, Phys. Rev. D **3**, 2153 (1971).
[40]S. Kamefuchi, L. O'Raifeartaigh, and A. Salam, Nucl. Phys. **28**, 529 (1961).
[41]P. van Nieuwenhuizen, Phys. Rep. **68**, 189 (1981).
[42]H. Tanebe and K. Ohta, Phys. Rev. C **31**, 1876 (1985).
[43]S. N. Yang, J. Phys. G **11**, L205 (1985).
[44]B. Blankleider, T.-S. Lee, and S. Nozawa, in *Excited Baryons 1988* (Ref. 1), pp. 288–292.
[45]K. M. Watson, Phys. Rev. **95**, 228 (1954). For a recent discussion of the Compton contribution, see M. Benmerrouche and N. C. Mukhopadhyay (unpublished).
[46]R. D. Peccei, Phys. Rev. **176**, 1812 (1968). G. Kramer, *ibid.* **171**, 2515 (1969); B. Dutta-Roy, I. R. Lapidus, and M. J. Tausner, *ibid.* **177**, 2529 (1969).
[47]S. Weinberg, Physica **96A**, 327 (1979).
[48]M. G. Olsson and E. T. Osypowski, Nucl. Phys. **B101**, 136 (1975).
[49]P. Noelle, Prog. Theor. Phys. **60**, 778 (1978).
[50]J. S. Ball, R. Campbell, P. S. Lee, and G. L. Shaw, Phys. Rev. Lett. **28**, 1143 (1972); J. S. Ball, P. S. Lee, and G. L. Shaw, Phys. Rev. D **7**, 2789 (1973); T.-Y. Cheng and D. B. Lichtenberg, *ibid.* **7**, 2249 (1972).
[51]R. Cenni, G. Dillon, and P. Christillin, Nuovo Cimento **97A**, 1 (1987).
[52]D. Menze, W. Pfeil, and R. Wilcke, Bonn compilation of pion photoproduction data (unpublished); most of the cross-section data may be found in the following articles: G. Fischer, H. Fischer, M. Heuel, G. von Holtey, G. Knop, and J. Stumpfig, Nucl. Phys. **B16**, 119 (1970); H. Genzel, E. Hilger, G. Knop, H. Kemen, and R. Wedemeyer, Z. Phys. **268**, 43 (1974).
[53]V. A. Get'man *et al.*, Nucl. Phys. **B188**, 397 (1981).
[54]A. A. Belyaev *et al.*, Yad. Fiz. **35**, 693 (1982) [Sov. J. Nucl. Phys. **35**, 401 (1982)].
[55]J. Stroer and R. Bulissch, *Introduction to Numerical Analysis* (Springer, New York, 1980), p. 39.
[56]Isgur, Karl, and Konuik (Ref. 5).
[57]Attempts have been made in some models to compare directly with the data. See, for example, M. Araki and A. N. Kamal, Phys. Rev. D **29**, 1345 (1984); M. Weyrauch, *ibid.* **35**, 1547 (1987).
[58]J. D. Bjorken and S. D. Drell, *Relativistic Quantum Mechanics* (McGraw-Hill, New York, 1964).